Neogene kinematics of the Giudicarie Belt and eastern Southern Alpine orogenic front (Northern Italy)

Vincent F. Verwater[1], Eline Le Breton[1], Mark R. Handy[1], Vincenzo Picotti[2], Azam Jozi Najafabadi[3], Christian Haberland[3]

[1]Institut für Geologische Wissenschaften, Freie Universität, Berlin, Germany
[2]Department of Earth Sciences, ETH-Zürich, Switzerland
[3]German Research Centre for Geosciences, GFZ, Potsdam, Germany

Correspondence to: Vincent F. Verwater (vincent.verwater@fu-berlin.de)

Abstract

Neogene indentation of the Adriatic plate into Europe led to major modifications of the Alpine orogenic structures and style of deformation in the Eastern and Southern Alps. The Giudicarie Belt is a prime example of this, as it offsets the entire Alpine orogenic edifice; its activity has been kinematically linked to strike-slip faulting and lateral extrusion

5 of the Eastern Alps. Remaining questions on the exact role of this fold-and-thrust belt in the structure of the Alpine orogen at depth necessitate a quantitative analysis of the shortening, kinematics and depth of decoupling beneath the Giudicarie Belt and adjacent parts of the Southern Alps. Tectonic balancing of a network of seven cross sections through the Giudicarie Belt parallel to the local NNW-SSE shortening direction reveals that this belt comprises two kinematic domains that accommodated different amounts of shortening during overlapping times. These two domains

10 are separated by the NW-SE oriented strike-slip Trento-Cles – Schio-Vicenza fault system, which offsets the Southern Alpine orogenic front in the south and merges with the Northern Giudicarie Fault in the north. The SW kinematic domain (Val Trompia sector) accommodated at least ~18 km of Late Oligocene to Early Miocene shortening. Since the Middle Miocene, this domain experienced at least ~12-22 km shortening, whereas the NE kinematic domain accommodated at least ~25-35 km shortening. Together, these domains contributed an estimated minimum of ~40-47

15 km of sinistral strike-slip motion along the Northern Giudicarie Fault, implying that most offset of the Periadriatic Fault is due to Late Oligocene to Neogene indentation of the Adriatic plate into the Eastern Alps. Moreover, the faults linking the Giudicarie Belt with the Northern Giudicarie Fault reach ~15-20 km depth, indicating a thick-skinned tectonic style of deformation. These fault detachments may also connect at depth with a lower crustal Adriatic wedge that protruded north of the Periadriatic Fault and was responsible for N-S shortening and eastward, orogen-parallel

20 escape of deeply exhumed units in the Tauer Window. Finally, the east-west lateral variation of shortening across the Giudicarie Belt indicates internal deformation and lateral variation in strength of the Adriatic indenter related to Permian - Mesozoic tectonic structures and paleogeographic domains.

1   Introduction

The fold-and-thrust belt of the eastern Southern Alps formed due to indentation of the Adriatic plate into the Eastern Alps (Schönborn, 1992; 1999; Picotti et al., 1995; Frisch et al., 1998; 2000; Castellarin and Cantelli, 2000; Linzer et al., 2002; Rosenberg et al., 2007; Pomella et al., 2011; 2012; Favaro et al., 2017). Indentation is defined as the post-collisional penetration of a relatively stiff part of an upper plate into a weaker, already existing orogenic edifice (e.g., Tapponier et al., 1986). In the Alps, indentation modified the early Tertiary nappe structure of the orogen (Schmid et al., 2004), including post-nappe folding and exhumation of Alpine metamorphic units in the Tauern Window (Rosenberg et al., 2018), eastward lateral extrusion of the Austroalpine nappes (Ratschbacher et al., 1991; Rosenberg et al., 2007; Scharf et al. 2013) and south-directed folding in the Southern Alps (Doglioni and Bosellini 1987; Castellarin et al. 2006b). The Giudicarie Fault, subdivided into a northern (NGF) and a southern (SGF) branches, is a prominent structure that offsets sinistrally the Periadriatic Fault (PF) by ~75 km in map view (Fig. 1). It ends to the north at the western boundary of Neogene post-nappe folding of the Tauern Window and lateral escape of the Eastern Alps (Frisch et al., 2000; Linzer et al., 2002; Scharf et al., 2013). Previous studies have established a direct kinematic link between sinistral motion along the NGF and Neogene exhumation in the Tauern Window (Ratschbacher et al., 1989; Frisch et al., 1998; 2000; Linzer et al., 2002; Rosenberg et al., 2007 Scharf et al., 2013; Schmid et al., 2013; Handy et al., 2015; Favaro et al., 2015, 2017; Hülscher et al., 2021). This complex response of the orogenic crust to indentation calls for detachment of both sedimentary cover and metamorphic units above one or more detachments located at or above the Moho-discontinuity (Oldow et al., 1990). To the south, the Giudicarie fold-and-thrust belt trends obliquely to the dominantly south-verging thrusts in the Southern Alps and consists of (1) N-S to NNE-SSW trending thrusts and strike-slip faults and (2) E-W trending thrusts (e.g. Valsugana Fault and Southern Alps orogenic front; Fig. 1). The question arises of how oblique-sinistral shortening accommodated by the Giudicarie Belt is linked to Neogene displacements on the Giudicarie Fault, the Periadriatic Fault and in the Tauern Window. In particular, the kinematic link of this belt to the northern and southern segments of the Giudicarie Fault remains poorly constrained and is the focus of this study.

The Giudicarie Fault coincides also with significant changes in the mantle structure, as imaged by tomographic P-wave models that show a SE-dipping slab anomaly beneath the Central Alps and a steeply dipping enigmatic slab anomaly beneath the Eastern Alps (Lippitsch et al., 2003, Mitterbauer et al. 2011; Karousova et al. 2012). The model of Lippitsch et al. (2003) shows that the slab anomaly beneath the Eastern Alps dips towards the NNE, which would suggest a subduction of the Adriatic plate, with a length varying from 50 km in the west to 210 km in the east. The exact dip, length and plate tectonic affinity (Adriatic, European or mixed) of this slab anomaly remains however under strong debate (Mitterbauer et al., 2011; Handy et al., 2015; Qorbani et al., 2015; Kästle et al., 2020). Any amount of Adriatic subduction should be reflected in both Neogene shortening estimates across the eastern Southern Alps and Neogene estimates of lateral extrusion of the Eastern Alps. Proposed estimates for the amount of shortening across the Giudicarie Belt and Southern Alps range from 30 to 100 km (Laubscher, 1990; Doglioni, 1992; Roeder, 1992; Schönborn, 1992; 1999; Picotti et al., 1995; Castellarin and Cantelli, 2000; Nussbaum, 2000). This wide range reflects the complexity in the kinematics and strain partitioning between thrusts and strike-slip faults within the Giudicarie

65 Belt. Therefore, this study aims to provide new constraints on the kinematics of shortening within the Giudicarie Belt, as well as on the depth of deformation within the Adriatic indenter, to discuss its relationships to Neogene exhumation in the Tauern Window and lateral extrusion in the Eastern Alps. To do so, we first review the Permian to Jurassic pre-existing structures and paleogeography of the eastern Southern Alps that affect the kinematics and partitioning of the deformation related to the Alpine Orogeny (Sect. 2). Structural observations on the field (Sect. 3) and deformation
70 ages (Sect. 4) along the Giudicarie belt are then used to construct a series of balanced geological cross-sections (Sect. 5). Based on the calculated amount of shortening, we propose a kinematic sub-division of the Giudicarie Belt (Sect. 6) and discuss the relationship between Neogene shortening along the Giudicarie Belt and Neogene motion along the NGF, a topic which has fascinated many researchers in the past (Castellarin and Vai, 1981; Picotti et al., 1995; Prosser; 1998, 2000; Müller et al., 2001; Viola et al., 2001; Linzer et al., 2002; Stipp et al., 2004; Pomella et al., 2011; 2012).

75
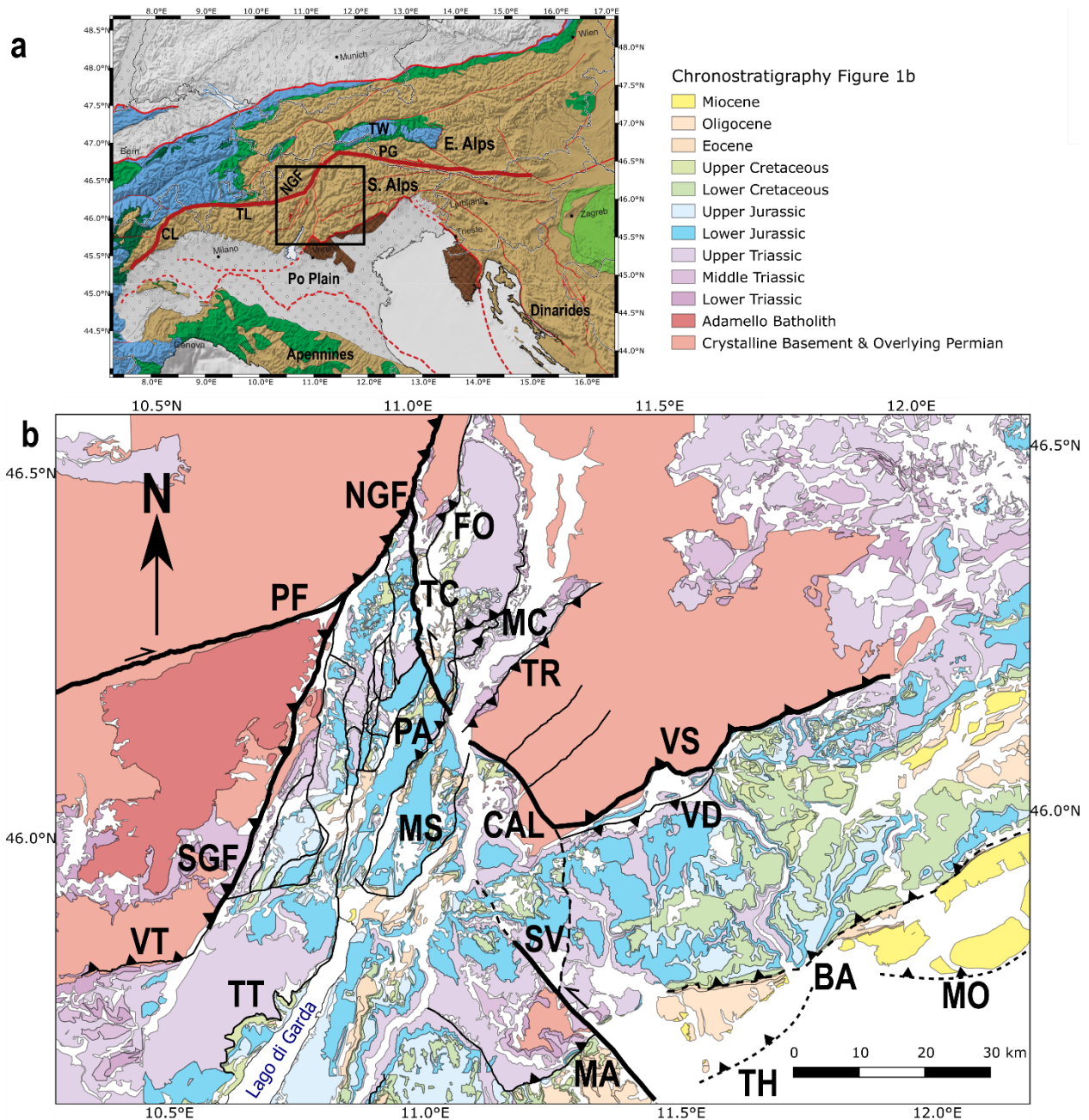
Figure 1: (a) Tectonic provenance map of the Alps (Handy et al., 2010 simplified from Schmid et al., 2004; 2008). The Southern Alps and Dinarides are accreted units derived from the Adriatic plate (brown). The Southern Alps are bounded to the north by the Periadriatic Fault (PF), which is sinistrally offset by the Northern Giudicarie Fault (NGF). The PF is divided into a western segment (Tonale and Canavese Lines, TL and CL, respectively) and eastern segment (Pusteria-Gailtal Line, PG). (b) Geological map of our study area (Giudicarie Belt) in the eastern Southern Alps indicated by a black square in (a). Abbr.: TW=Tauern Window; Fault abbreviations: BA=Bassano, CAL=Calisio, FO=Foiana, MA=Marana, MC=Mezzocorona, MO=Montello, MS=Monte Stivo, PA=Paganella, SGF=Southern Giudicarie, SV=Schio-Vicenza, TC=Trento-Cles, TH=Thiene-Bassano Fault, TR=Truden, TT=Tremosine-Tignale, VD=Val di Sella, VS=Valsugana, VT=Val Trompia.

2   Geological setting

2.1   The eastern Southern Alps

The Southern Alps are a predominantly south-vergent fold-and-thrust belt, at the leading edge of the Adriatic plate indenting the European plate to the north. The Giudicarie Fault is the boundary between eastern and western parts of the Southern Alps (Schönborn, 1999; Castellarin and Cantelli, 2000). In the Late Cretaceous, the tectonic regime shifted in the Alps from E-W extension to N-S shortening due to convergence between Adria and Europe (e.g., Dewey et al. 1989). The western Southern Alps record a Late Cretaceous compressional phase (documented by the so-called Lombardian Flysch; e.g. Doglioni and Bosellini, 1987; Bernoulli and Winkler, 1990; as well as thrusting that pre-dates the Paleogene Adamello intrusive body, see Brack, 1981) followed by Oligocene to Middle Miocene shortening (e.g. Schönborn, 1992; Schmid et al., 1996). Only the western Southern Alps have recorded this Late Cretaceous deformation (Castellarin et al., 1992), as within the eastern Southern Alps evidence of this phase is lacking. The eastern Southern Alps comprise actively accreting cover units of the Adriatic plate and are bounded to the north by the PF, to the west by the NGF and SGF, to the east by Dinaric thrusts and active strike-slip faults, and to the south by the Po Plain (Fig. 1). Paleostress analyses (Castellarin et al., 1992; Castellarin and Cantelli, 2000; Zampieri et al., 2003) and structural analysis of the NGF (Prosser, 1998; 2000; Viola et al., 2001) show that during the Middle to Late Miocene, the eastern Southern Alps were dominantly affected by NNW-SSE shortening, which reactivated many Permo-Jurassic faults. This Neogene NNW-SSE shortening was preceded by a minor phase of Eocene E-W extension related to the opening of a volcanic graben, which was only recorded locally in the southernmost part of the Trento Platform (Zampieri, 1995).

Directly north of the Giudicarie Belt and Periadriatic Fault, nappes in the Tauern Window were affected by km-scale upright folding and orogen-parallel extrusion towards the Pannonian Basin in Miocene time (Ratschbacher et al., 1991; Frisch et al., 1998; Scharf et al., 2013). The northern Alpine front west of Munich (northwest of the Tauern Window) was active until the Pliocene (Von Hagke et al., 2012), whereas east of Munich it ceased propagating northwards after ~20 to 15 Ma (Ortner et al., 2015). This cessation coincides broadly with the onset of sinistral transpression along the Giudicarie Belt, as well as south-directed thrusting in the eastern Southern Alps (Castellarin and Cantelli, 2000; Schmid et al., 2013 and references therein). During this time, rapid exhumation of Penninic and Subpenninic nappes in the Tauern Window commenced (Fügenschuh et al., 1997), although slower exhumation in the Tauern Window may already have started earlier, in the late Oligocene time (Pomella et al., 2012; Scharf et al., 2013; Favaro et al., 2015). Taken together, these events have been interpreted to indicate that Adriatic indentation triggered the orogen-parallel extrusion of the Eastern Alps towards the Pannonian Basin (Ratschbacher et al., 1989; Frisch et al., 1998; 2000; Linzer et al., 2002; Rosenberg et al., 2007; Favaro et al., 2017). Contrasting estimates have been proposed for the amount of lateral extrusion, ranging from 14-62 km (Rosenberg and Garcia, 2011; disputed by Fügenschuh et al., 2012), 65-77 km (Favaro et al., 2017), 100 km (Scharf et al., 2013), to as much as 120 km (Linzer et al., 2002) and 160 km (Frisch et al., 2000).

The NGF and its northern prolongation, the Meran Mauls Fault, sinistrally offset the PF by 75 km, dividing the PF into the Tonale Line (western segment) and the Pusteria Line (eastern segment; Fig. 1). Discussion has focused on whether the NGF is an exclusively Neogene fault that sinistrally offsets a formerly straight PF, or if the NGF formed a pre-Neogene bend of the PF that was reactivated under transpression during the Neogene (Castellarin and Vai, 1981; Picotti et al., 1995; Prosser; 1998, 2000; Müller et al., 2001; Viola et al., 2001; Linzer et al., 2002; Stipp et al., 2004; Pomella et al., 2011; 2012). The latter hypothesis is supported by Picotti et al. (1995), who estimated that the amount of strike-slip (30-40 km) along the NFG, extrapolated from the amount of Neogene shortening calculated within the southwestern part of the Giudicarie Belt, was less than the 75 km offset of the PF. In addition, several studies (e.g. Doglioni and Bosellini, 1987; Castellarin et al., 2006b) have interpreted the lateral termination of the Cretaceous pre-Adamello deformation phase along the NGF, as a late Cretaceous lateral ramp. However, the interpretation of a pre-Neogene offset PF is incompatible with the proposed 100-150 km of Paleogene dextral strike-slip along this fault (Laubscher, 1991; Schmid and Kissling, 2000) based on offset correlative features on either side of it, i.e. the Ivrea- and Pejo-zones (Laubscher, 1991) and the Sesia-Dent Blanche and Margna units (Laubscher 1991; Schmid et al., 1996; Handy et al., 2005). In addition, a paleomagnetic study of Pomella et al. (2011) convincingly shows that the Periadriatic granitoid intrusions along the NGF underwent counterclockwise rigid-body rotation into their current NNE-SSW striking orientation in Neogene time, suggesting the NGF can be interpreted as a rotated segment of the PF (Pomella et al., 2011; 2012). Although a paleomagnetic study across the Southern and Eastern Alps possibly indicates a larger-scale coherent Oligocene to Miocene rotation rather than a local reorientation (Thöny et al., 2006). Potential links between Neogene shortening in the Giudicarie Belt and strike-slip motion across the NGF and adjacent Tonale and Pusteria fault segments are therefore of great relevance for a better understanding of Neogene collision processes in the Eastern and Southern Alps.

To assess the amount of Neogene shortening within the eastern Southern Alps, it is important to constrain the role of inherited Permian to Mesozoic structures. Indeed, many of the Neogene fault structures were inherited from earlier tectonic events, which include Permian to Jurassic rifting phases (Handy, 1987; Handy and Zingg, 1991; Bertotti et al., 1993; Selli et al., 1996; Picotti and Cobianchi, 2017; Le Breton et al., 2021).

2.2   Permian to Jurassic paleogeography

Based on Permo-Mesozoic stratigraphic variations, we divide our study area into six different paleogeographical domains (Fig. 2) which, as we show below, exert important controls on the partitioning of Neogene shortening. Within the eastern Southern Alps, the Atesina Volcanic Complex (Fig. 2) is a good example of a Permian basin filled with volcanic sediments, with the Valsugana Fault interpreted as a dextral Permian feature (Zampieri et al., 2003) and the Calisio and Truden faults recording a Permian normal faulting history (Selli et al., 1996). Another minor unit in the eastern Southern Alps containing evidence of this interpreted Permian transtensional phase (Zampieri et al., 2003) is exposed in the hanging wall of the Foiana Fault (Fig. 1).

From the Late Triassic to Jurassic, a rifting related to the opening of the Alpine Tethys west and north of Adria (Piemont-Liguria Ocean) affected the Adriatic plate (e.g. Handy, 1987; Handy and Zingg, 1991; Bertotti et al., 1993; Picotti and Cobianchi, 2017; Le Breton et al., 2021). The rifting of Alpine Tethys led to the formation of carbonate platforms and basins bounded by N-S trending faults that are still well preserved within the Southern Alps (Bernoulli and Jenkyns, 1974; Winterer and Bosellini, 1981). The main N-S trending faults divided the area into four different domains from west to east (Bernoulli and Jenkyns, 1974; Winterer and Bosellini, 1981): the Lombardian Basin, the Trento Platform, the Belluno Basin and the Friuli Platform (Fig. 2). The Lombardian Basin recorded the most Triassic to Jurassic subsidence (Winterer and Bosellini 1981; Bertotti et al., 1993), reaching ~5 km of sedimentary thickness, and is bounded in the east by the Ballino-Garda and Tremosine-Tignale Faults (Fig. 1 and 2). Differential subsidence caused significant stratigraphic thickness variations within the Jurassic paleogeographic domains (Picotti et al., 1995). Within the Trento Platform, thicknesses decrease from ~3 to ~2 km both towards the SE and NE dividing the Trento Platform itself into sub-domains: the Trento Platform (numbered 2 on Fig. 2), the Reduced Recoaro High (2a), the Reduced Trento Platform (2b), the Atesina Volcanic Complex (2c) and the Asiago Plateau (2d). These thickness variations broadly coincide with Neogene faults, including the Trento-Cles Fault, Truden Fault, Calisio Fault, Valsugana Fault and Schio-Vicenza Fault (Fig. 1 and 2). The Atesina Volcanic Complex forms the most prominent Permian paleogeographical domain with a 2 km thick Permian sequence, with no overlying Triassic to Cretaceous sedimentary cover outcropping (Fig. 2). It is assumed that the Atesina Volcanic Complex (domain 2c) had a similar Mesozoic cover as the nearby and paleogeographically comparable Reduced Trento Platform (2b) (Selli, 1998), which was later eroded in the Miocene. This assumption is based on the observation of Mesozoic clasts found in Miocene conglomerates in the footwall of the Valsugana Fault (Castellarin et al., 1992). Another paleogeographic domains containing thinner Permian volcanic successions (up to ~1 km thick; Fig. 2) is the Reduced Trento Platform. Further small-scale thickness variations across Mesozoic faults occur within the paleogeographic domains defined here (Franceschi et al., 2014). However, these are beyond the aim of this paper and are neglected in order to simplify the construction and balancing of cross sections (Sect. 5).
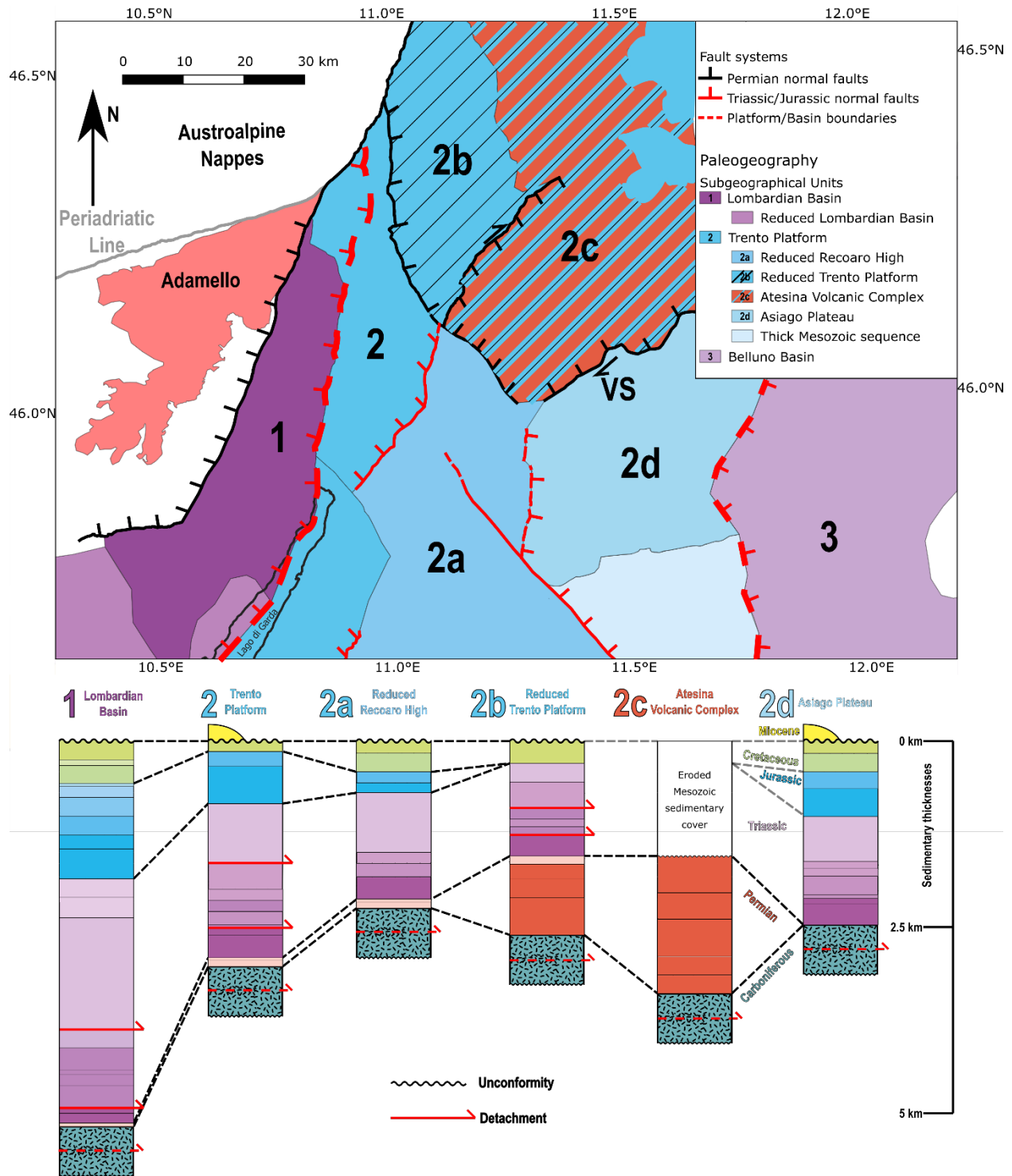
Figure 2: Triassic to Jurassic paleographic basinal (1, Lombardian Basin; in violet) and platform domains (2, Trento Platform in blue). Based on Mesozoic thickness variations, the Trento Platform is subdivided into units 2a-d. Note that within domain 2c no Mesozoic sediments are exposed and the thickness of the eroded Mesozoic sequence is extrapolated from domain 2b, based on the occurrence of Miocene conglomerates with Mesozoic clasts unconformably overlying Mesozoic strata in domain 2d. Domain 2 also includes a Cenozoic sequence unconformably overlying Mesozoic strata outcropping at Monte Brione (see discussion Sect. 4). Simplified stratigraphic columns (below) for each paleogeographic domain 1-2d.

185

3   Structural observations and fault-slip analysis

Structural data from the eastern Southern Alps were collected as input for fault-slip analysis to calculate the main Neogene shortening direction. This was necessary to estimate the amount of shortening parallel to the shortening direction in the balanced cross sections. Special attention was paid to fault systems coinciding with paleographic variations (the Trento-Cles, Calisio, Valsugana and Schio-Vicenza Faults; Fig. 1, 2, 3 and 4) to test if these features coincide with variations in structural style and amount of shortening.

Structural analysis in the Giudicarie-Valsugana sector of the eastern Southern Alps included measuring fault surfaces, their striations and shear-sense, fold-axial planes, as well as bedding planes near folds and faults. These data formed the input for fault-slip analysis, which was performed in the WinTensor software version 5.8.8 (Delvaux and Sperner, 2003). An angle of 30° between the maximum principal stress and the shear plane based on the Mohr-Coulomb failure criterion was assumed. However, given the proximity of the measured fault striations to major fault structures (Fig. 4), this angle might have been different due to strain complexities. The maximum principal stress sigma-1 was calculated in the WinTensor software for various fault systems, assuming that structures measured in the field reflect the principal incremental strain direction and principal stress direction sigma-1. The final stereoplots with results of the fault-slip analysis calculated with WinTensor were drawn using FaultKin 8.0.0 software (Fig. 4; Marrett and Allmendinger, 1990).

Bedding and striation measurements (Fig. 3) were collected along the Bassano (Fig. 3a) and Marana (Fig. 3b) thrust faults on either side of the Schio-Vicenza Fault (Fig. 3c, 3d and 3e) to test for variations in structural style. The Schio-Vicenza Fault represents an inherited Mesozoic feature associated with stratigraphic thickness variations (Fig. 2). Along the Borcola Pass Fault zone, a branch of the Schio-Vicenza Fault, steeply dipping NW-SE to N-S trending fault surfaces containing sinistral striations cut Eocene mafic dikes (Fig. 3c and 3d). Striation steps indicating sinistral motion related to local NNW-SSE incremental strain (Fig. 3d) parallel to the main shortening direction (Castellarin and Cantelli, 2000) indicate that the Schio-Vicenza Fault was reactivated during post-Eocene time. These striations are overprinted by younger striations indicating downthrow of the NE-block (Fig. 3e) that are interpreted to be related to flexural extension of the foreland bulge of the Apennines (Pola et al., 2014). Contrasting deformation styles east and west of the fault may indicate that the Schio-Vicenza Fault acted as a transfer fault. Indeed, directly east of the Schio-Vicenza Fault, strata in the hanging wall of the Bassano Fault (Fig. 1) are steeply dipping, strongly folded and form the forelimb of the ENE-WSW trending Monte Grappa ramp anticline (Fig. 3a), whereas to the west, the Marana thrust emplaces cataclastically deformed Norian Dolomia Principale on Hettangian to Pliensbachian Calcari Grigi (Fig. 3b). We note that in the hanging wall of the Marana thrust, a deeper structural level is exposed than in the hanging wall of the Bassano Fault, implying that the observed variation in structural style may partly be due to a different erosional level. Variability in the geometry at depth of the Bassano and Marana Faults (see discussion in Sect. 5.2) are the cause of the observed contrasting structural styles. The deeper level of exposure along the Marana thrust and the southern part of domain 2a (Fig. 2) has been interpreted to indicate that this area represents a structural high (prolongation of the Adige embayment in Laubscher, 1990). No thrust associated with the Monte Grappa ramp

anticline is exposed; the anticline is therefore interpreted as a fault-propagation fold above the blind Bassano Fault, in agreement with earlier studies (Doglioni, 1990; Roeder, 1992; Pilli et al., 2012; Pola et al., 2015). The Schio-Vicenza Fault is only observed as far north as the Adige Valley. However, previous studies argued for either a continuous Trento-Cles – Schio-Vicenza (TC-SV) fault system (Semenza, 1974) or a contractional strike-slip stepover with the

230   Calisio Fault connecting the Trento-Cles and Schio-Vicenza Faults (Zampieri et al., 2003; Zampieri et al., 2021). The TC-SV fault system will be further discussed in Sect. 5 and 6.

Strike-slip deformation along the Schio-Vicenza Fault ends towards the NW in the vicinity of the Valsugana Fault (Fig. 1). This fault was reactivated as a Neogene thrust and emplaced Variscan basement onto Mesozoic sediments of

235   the Trento Platform in its western part and Triassic onto Jurassic strata in the east. Striations in the field measured along faults conjugate to the main trend of the Valsugana show thrust motion with components of dextral (Fig. 3f) and sinistral strike-slip. Fault-slip analysis on these striations (Fig. 4) is consistent with NNW-SSE shortening, exactly perpendicular to the main Valsugana Fault trend. Therefore, we interpret that there was no significant component of Neogene strike-slip motion along the Valsugana Fault. The lateral ramp of the Valsugana Fault is the Calisio Fault

240   (Fig. 1), which merges with the Trento-Cles Fault, thereby inverting a major Permian paleographic boundary (Fig. 2). Striations from the Valsugana, Marana, Bassano and Schio-Vicenza faults, ENE-WSW trending axial planes and axes of the Monte Grappa ramp anticline, and striations in the footwall of the Marana Fault and results from a literature compilation (Fig. 4) are all consistent with NNW-SSE shortening.

245 **Figure 3:(a) Steepened Lower Cretaceous strata (Majolica), which are commonly found in the forelimb of the Monte Grappa ramp anticline forming the hanging wall of the blind Bassano Thrust. The black dashed lines indicate fold axes of chevron folds (formed due to flexural slip); (b) The Marana Thrust at Zanconati emplaces Norian Dolomia Principale on Lower Jurassic Calcari Grigi; (c) The Schio-Vicenza Fault at Passo della Borcola, offsetting Norian Dolomia Principale and Eocene mafic dykes. Striations on fault surfaces indicate oblique sinistral down-dip motion; (d) Older striations on the**

250 **Borcola Pass Fault Zone (BPFZ; after Fondriest et al., 2012) indicating sinistral sense of motion. (e) Younger striations on the BPFZ indicating oblique downthrow of the NE-block of the BPFZ. (f) Dextral strike-slip slickenfibres at the eastern end of the hanging wall of the Valsugana Fault (near Pieve di Cadore) where the Valsugana Fault branches into several fault splays and becomes transpressive. The uninterpreted field photographs can be found in the Supplement.**

255
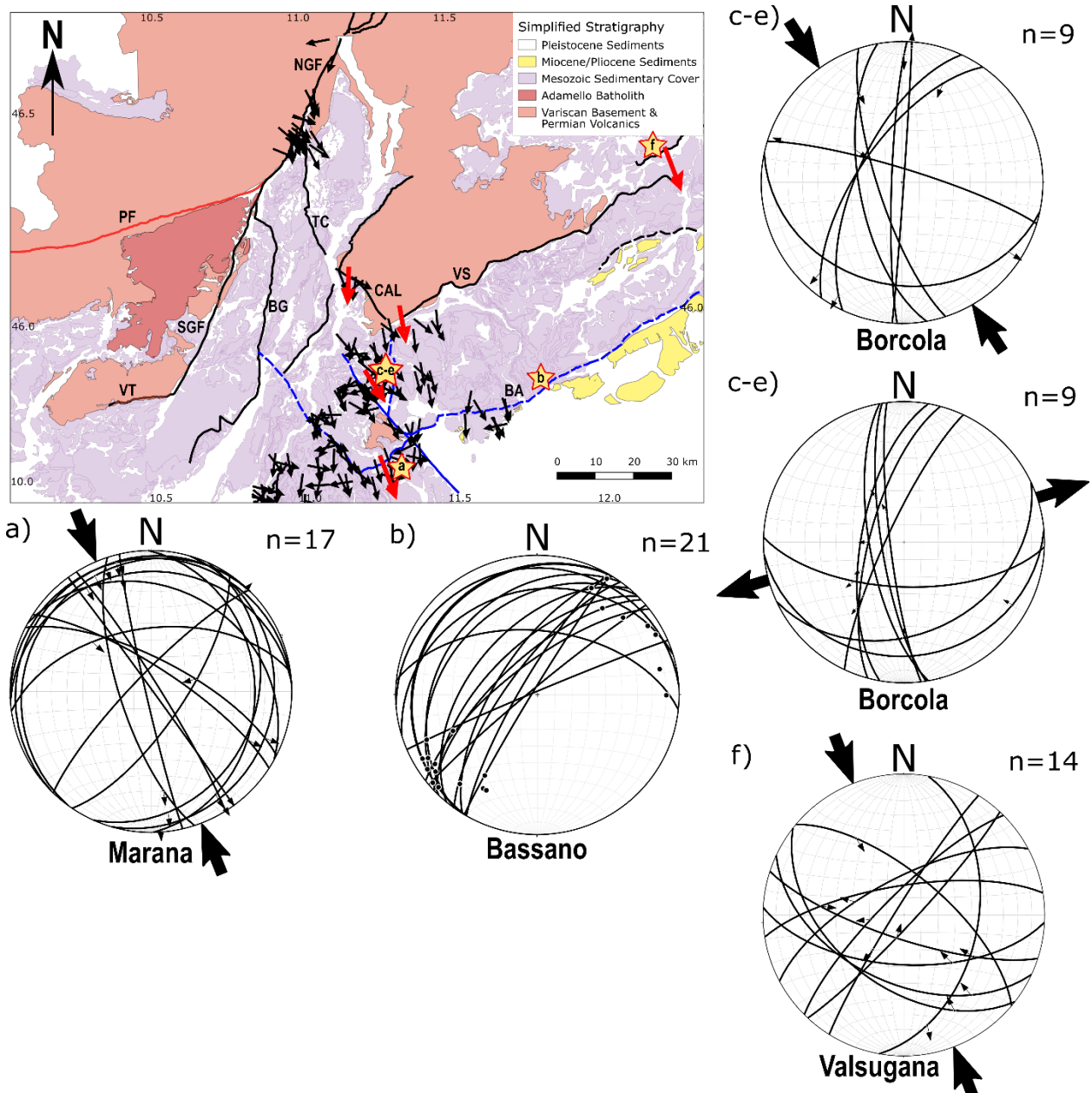
Figure 4: Structural map of the eastern Southern Alps showing the distribution of fault slip data from this study (in red; locations a-e indicated by stars on the map) and from the literature (in black). The geological map is a compilation of own field data and published geological maps (Bartolomei et al., 1967; Bosellini et al., 1967; Castellarin et al., 1968; 2005; Braga et al., 1971; Dal Piaz et al., 2007; Avanzini et al., 2010). See Fig. 1 for fault abbreviations. The field data includes fold axes

260 plotted on their fold axial planes for the Bassano Fault (b) and fault-slip analyses with local paleostrain directions for the Marana (a), Valsugana (f) and Borcola (c-e) faults. Two distinct stereoplots are shown for Borcola as two generations of striations are observed here (see discussion in Sect. 3). Regional (Castellarin and Cantelli, 2000; Zampieri et al., 2003) and local (Prosser, 1998; 2000; Viola et al., 2001) paleostrain analyses from the literature are indicated in black. The data indicate a dominant NNW-SSE shortening direction.

4 Age of deformation in the eastern Southern Alps

Individual thermochronological dated faults within the eastern Southern Alps include the NGF, SGF, Valsugana and Val Trompia faults, which are broadly coeval with stratigraphic age constraints indicating Neogene deformation (Fig. 5). Deformation in the eastern Southern Alps initiated during late Oligocene time (27.8-23.0 Ma), indicated by a detailed seismic survey beneath the Po Plain that documented Chattian to Burdigalian deposits affected by Late Oligocene to Neogene thrusts sealed by Messinian strata (e.g. Fantoni and Franciosi, 2010; and references therein).

A maximum age for the onset of thrusting within the Giudicarie Belt itself is given by the youngest sediments below a thrust that accommodated NNW-SSE shortening. At Monte Brione, at the northern end of Lake Garda (Fig. 1), the base of an arenitic-pelitic sequence dated at 21.5 Ma (Luciani and Silvestrini, 1996) shows westward divergent onlaps suggestive of growth in a footwall syncline (Castellarin et al., 2005). Directly east of Monte Brione, similar stratigraphic age constraints are found within deformed sediments of 28-16 Ma in the footwall of the Monte Stivo thrust (Fig. 5). Yet further to the east in the footwall of the Valsugana Fault, deformed Serravallian (~14-12 Ma) sediments date south-directed thrusting (Castellarin et al., 1992; Selli, 1998). Similar ages (17-9 Ma) were obtained with apatite fission-tracks from the hanging wall of the Valsugana Fault and several faults along the Giudicarie Belt (Pomella et al., 2012; Heberer et al., 2016). This main phase of Neogene shortening has been termed the Valsugana Phase, and was coeval with shortening along the Giudicarie Belt (Castellarin et al., 1992; Castellarin and Cantelli, 2000). Several former Mesozoic structures were reactivated during the Valsugana phase, including the Schio-Vicenza Fault (Fig. 2). The final pulse of exhumation of the Valsugana phase occurred between 10 and 8 Ma, as shown by a study of Reverman et al. (2012) using (U-Th-Sm)/He and fission track thermochronology on apatites from the Adamello batholith.

A younger phase of Messinian to Pliocene shortening has been recognized along the Bassano and Montello faults of the Southern Alpine orogenic front (Massari et al., 1986; Castellarin et al., 1992). Late Tortonian to Early Pliocene fossils (Dal Piaz, 1912, Massari et al., 1986) are found in mudstones interbedded with conglomerates in a syn-tectonic wedge in the hanging wall of the Bassano and Montello Faults (Massari et al., 1986). Historical seismicity (e.g. Galadini et al., 2005) and clustering of (micro-)seismic hypocenters (Romano et al., 2019; Anderlini et al., 2020; Jozi Najafabadi et al., 2020) along these fault systems and morphological evidence of fault surface rupture (Moratto et al., 2019; Romano et al., 2019) indicate that this younger phase of shortening is still active.

The Adamello granitoids, the Variscan basement and overlying Permian volcanics are better suited for geochronological studies, as reflected in the clustering of age data within these rock units (Fig. 5). Early to Late Miocene thermochronological ages along the NGF (Viola et al., 2001; Pomella et al., 2011; 2012) and within the Val Trompia-sector of the Giudicarie Belt (Heberer et al., 2016; VT in Fig. 5) fall within the same age interval as the stratigraphic constraints above, indicating the coeval evolution of the NGF and Giudicarie Belt.

In addition, pre-Oligocene ages of shortening have been reported in the eastern Dolomites (Doglioni and Bosellini, 1987) based on similarities with Dinaric thrust directions and Oligocene deposits unconformably overlying Mesozoic strata (Doglioni and Bosellini, 1987; Keim and Stingl, 2000). However, these faults only occur east of our study area. West of the SGF, a pre-Adamello phase of shortening is recognized along the Val Trompia-sector of the Giudicarie

305   Belt (Brack 1981; Doglioni and Bosellini, 1987; Picotti et al., 1995; Castellarin et al., 2006b). Relative age constraints are provided here by the observation that the Gallinera Fault is cross-cut by the western side of the Adamello batholith (Brack, 1981; Picotti et al., 1995; Castellarin et al., 2006b), which indicates a pre-Adamello age of deformation, possibly Cretaceous. However, within our study area east of Adamello, no such indications for pre-Adamello deformation can be found. This suggests the presence of a Cretaceous lateral ramp between the western and the eastern

310   Southern Alps (Doglioni and Bosellini, 1987; Castellarin et al., 2006b).
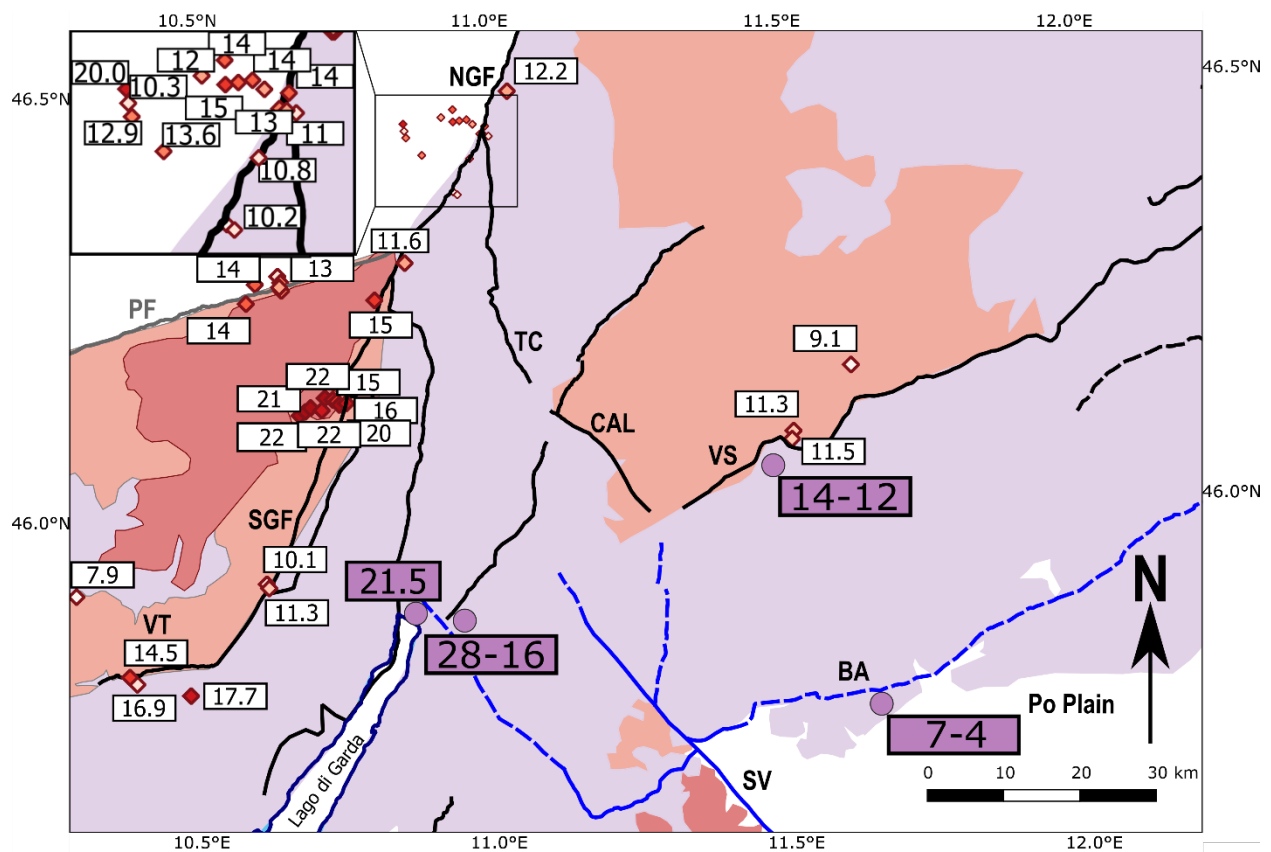
Figure 5: Compilation of stratigraphic and AFT age data in the eastern Southern Alps from Luciani and Silvestrini, (1996); Martin et al. (1998); Castellarin and Cantelli (2000); Viola et al. (2001); Stipp et al. (2004); Pomella et al., (2011; 2012); Heberer et al. (2016). Purple boxes mark biostratigraphic ages of deformed sediments (Castellarin et al., 1992). The inset

315   **map outlines the Adamello-Giudicarie area at the junction of the NGF and TC faults, with the locations of many, tightly spaced age data. See Fig. 1 for fault abbreviations.**

5   Shortening estimates and depth of detachment in the eastern Southern Alps

5.1   Assumptions for structural analysis and cross section balancing

All kinematic models of the Giudicarie Belt agree that deformation involved Neogene transpression with strain partitioning between strike-slip and thrust faults (Picotti et al., 1995; Prosser, 1998; 2000). To obtain reliable estimates of shortening across the belt, it is necessary to account for rock volumes moving into and out of 2-D sections traces. Seven cross sections were constructed parallel to the NNW-SSE Neogene direction of principle shortening direction obtained from fault-slip analysis above (Fig. 3e). These cross sections straddle the Schio-Vicenza, Trento-Cles and Ballino-Garda faults (Fig. 6), which as we have shown above, coincide with the main boundaries of paleogeographic domains (Fig. 2). In addition, seven perpendicular (orogen-parallel) cross sections were constructed to assess stratigraphic variations across these faults (Fig. 6). Stratigraphic and tectonic contacts were projected into the sections using structural contours constructed from published geological maps (Bartolomei et al., 1967; Bosellini et al., 1967; Castellarin et al., 1968; 2005; Braga et al., 1971; Dal Piaz et al., 2007; Avanzini et al., 2010). In addition, publicly available bore-hole data for the southern part of the studied area beneath the Po Plain (Paese, Scaldaferro, Travettore and Villaverla wells; VIDEPI-database) constrain the thickness of the sedimentary cover. Thickness variations within the paleogeographic domains of Fig. 2 are neglected and only variations across these major paleogeographic boundaries are incorporated in the cross sections. Thicknesses within the profiles were extrapolated to depth and above the current erosional level using the kink-band and dip-domain methods (Boyer, 1986).

Line-length balancing was performed with the Move software package (provided by Petex) using the flexural slip algorithm for unfolding the horizons. We assumed a flat top-Cretaceous horizon and used this as a marker to estimate the fault displacements. This is admittedly a simplification given the lateral facies and thickness variations in Cretaceous strata (Doglioni and Bosellini, 1987). Modelled fault geometries at depth were tested using a trial-and-error, forward modelling approach until a best-fit with the present-day surface geology was found. We assumed that all the observed folds along the profiles are fault-related and employed a fault-bend-fold algorithm (Suppe, 1983) in Move. This algorithm treats faults as brittle, discrete discontinuities, even at depths below ~10 km where ductile behavior is expected in natural systems. The fault-bend-fold algorithm maintains line length and area in forward modelling, in contrast to its alternative, fault-parallel flow, which only maintains line length when a correct angle of angular shear is specified. We avoided fault-parallel flow modelling because this angle is not well constrained in the studied area. It is inferred that the Northern Giudicarie Fault (NGF) forms the backstop of the south-vergent Neogene deformation of the eastern Southern Alps and that all interpreted detachments are connected at depth with the NGF. This is in line with the absence of any significant Neogene deformation in the Austroalpine basement to the NW of the NGF. It is clear that sinistral strike-slip motion of up to 75 km along the NGF itself was coeval with thrusting in the Giudicarie Belt (e.g., Pomella et al. 2011), but transpressional movement cannot be incorporated in the fault-bend-folding algorithm of Move. Thus, in forward modelling of all cross sections, the NGF is progressively offset as a passive marker along the fault detachments (Fig. 7, 8 and 9).

The 3D Move database including all 14 cross-sections, as well as descriptions of selected cross sections 1, 5, 6 and details on the forward modelling approach, are available as supplementary material in Verwater et al. (2021; see data availability section below). Regardless of the balancing methods employed here, all estimates of shortening must be regarded as minima. There are several basic reasons for this: (1) the cutoff lines of strata in the hanging wall of many thrusts have been eroded, such that markers for determining the full amount of displacement are lacking. This is particular true of the highest detachments in a thrust system, where erosion is greatest; (2) many detachments in the deeper levels of thrust systems are "blind", i.e., the displacement at their tips tends to zero at depths where constraints on the geometry of their propagation structures (e.g., folds) are poorly or even unconstrained. This is particularly the case where boreholes or seismic information are unavailable, as in the foreland of some of the thrust systems reported below; (3) In extreme cases, thrust systems can "cannibalize" their own deepest detachments, removing them to depths beyond detection with available seismic information. This type of tectonic erosion, especially in basement units with low impedance contrasts, will always lead to an underestimation of shortening; (4) out-of-section motion, as for example the sinistral strike-slip component in the Giudicarie Belt, necessarily renders 2D areal and line balancing inadequate for determining the true amount of shortening; (5) alternative structural interpretations involving duplexes and/or triangle zones at depth increasing the amount of shortening (see discussion in Sect. 5.2 and the supplementary material in Sect. Data Availability). We have attempted to compensate for this innate bias by balancing shortening in the aforementioned network of closely spaced cross sections, and in fact use the differences in minimum shortening estimates to judge the degree of transpression within the Giudicarie Belt (Sect. 6 below). Despite these limitations, the minimum shortening estimates allow us to place a lower limit on the amount of shortening parallel to the bulk shortening direction within the Giudicarie Belt.

5.2   Results of shortening estimates from cross-section balancing

Amounts of shortening in orogen-normal profiles vary laterally along the Giudicarie Belt (Fig. 6). To the south-west (Profiles 1 and 2), balancing yield 18-22 km of shortening. Similarly, to the northeast (Profiles 6 and 7), shortening estimates range from 17 to 25 km. However, shortening is only 8 to 12 km in the central part of the Giudicarie Belt (Profiles 3, 4, 5). The largest variation in shortening occurs between profiles 5 (11 km) and 6 (25 km) across the TC-SV fault system (Fig. 6, 8 and 9). We infer a dominantly thick-skinned style of deformation, with detachments reaching down to ~15 km depth based on exposure of basement in the hanging wall of steep thrusts, recent seismicity clustering at depths of 10 to 20 km (Viganò et al., 2015; Jozi Najafabadi et al., 2020) and forward modelling in Move (Figs. 6, 7, 8 and 9; Supplement in Verwater et al. 2021).

These minimum shortening estimates are fairly well constrained, as the fault displacement observed at the surface provides the most important constraint for the amount of shortening and uncertainties of fault structures at depth have errors of 2-3 km (see discussion supplementary material). Although the Giudicarie Belt exposes several long decollements within the sedimentary cover (e.g. Tremosine-Tignale, Paganella and Tosa Faults; Fig. 7 and 8), field observations show that, with the exception of the Mezzocorona antiformal stack along profile 6 (Fig. 9a), there are no

large-scale duplexes exposed. This suggests that kinematic models with several putative duplexes at depth are inconsistent with field observations. However, the geometries in the footwall of the Paganella (profile 5; Fig. 8) and Valsugana Faults (profile 6; Fig. 9) allow for alternative interpretations in which possible duplexes at depth are linked with shortening at the surface. These duplexes would increase shortening along profiles 5 and 6 by ~2 to 3 km (see alternative interpretations of profiles 5 and 6 in data repository of Verwater et al. 2021). The 3 km uncertainty in shortening along profile 5 is 27% of the total minimum amount of shortening observed along this profile and can also be taken as a percentage of uncertainty in the shortening estimates of the other profiles (Fig. 6). The presence of eroded hanging wall cutoffs along our profiles (Fig. 7, 8 and 9) could yield additional errors in our shortening estimates, further increasing the 27% uncertainty. In addition, the clustering of seismic events along modelled fault structures in the basement propagating southward in profiles 1, 5 and 6 (Fig. 7, 8 and 9; Jozi Najafabadi et al., 2020) is consistent with thick-skinned tectonics featuring ramps that root in the basement units.

Profile	1	2	3	4	5	6	7
Shortening	18 km	22 km	8 km	12 km	11 km	25 km	17 km
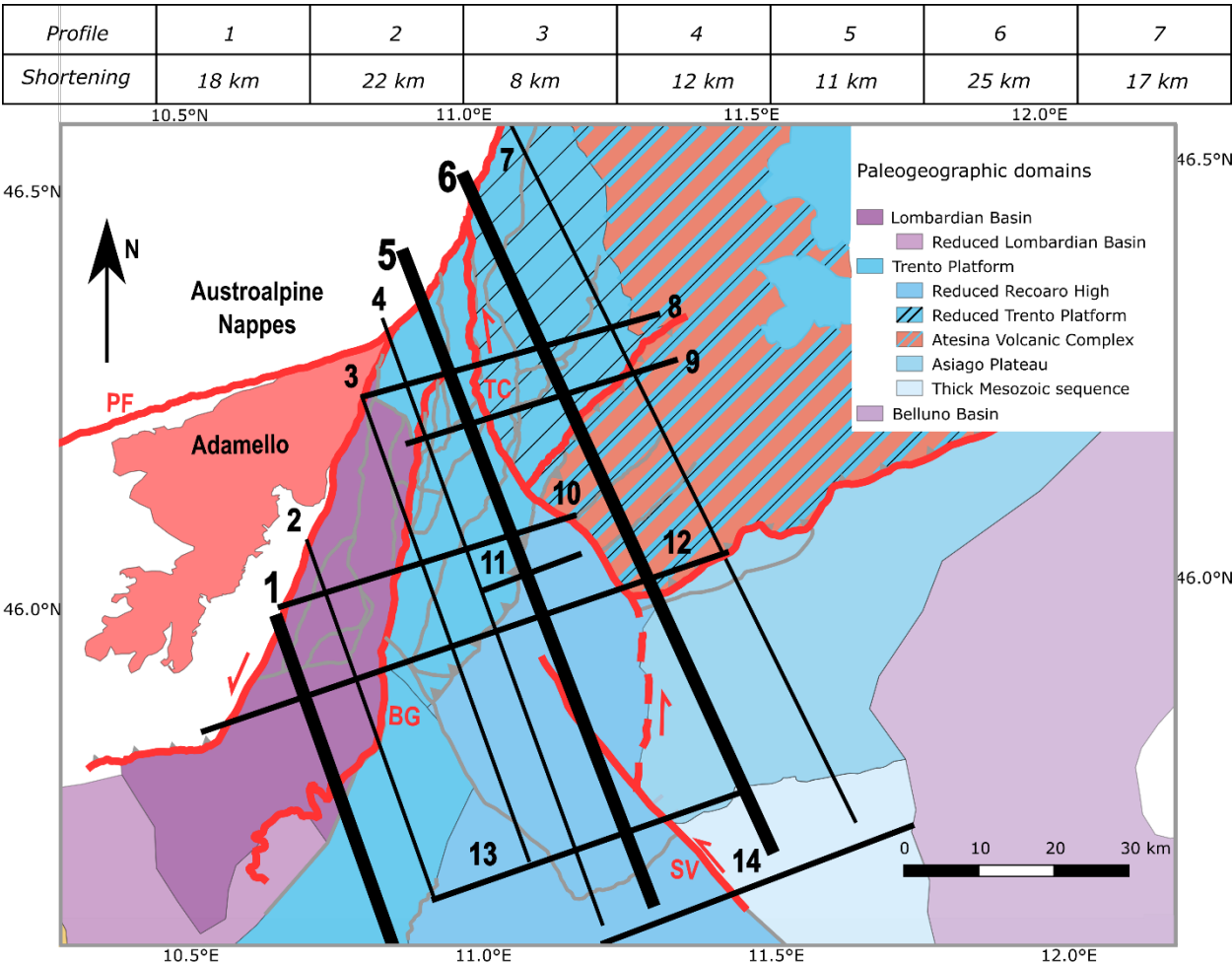
Figure 6: Traces of cross sections constructed and balanced in this study. Details of profile reconstructions for profiles 1, 5 and 6 (thick black lines) is shown on Fig. 7, 8 and 9, respectively. Profiles not shown in Fig. 7, 8, 9 and 10 are available in the supplementary material. Abbr. BG: Ballino-Garda Fault; PF=Periadriatic Fault; SV: Schio-Vicenza Fault; TC: Trento-Cles Fault.

5.3 Forward modelling of fault detachments at depth

Sub-surface faults in profiles 1-7 (Fig. 7, 8, 9 and 10) were determined from forward modelling of an initial undeformed state involving layer-cake stratigraphy (Fig. 7b, 8b and 9b). This assumption is necessary for balancing, though in light of the aforementioned Mesozoic rifting in this area (Sect. 3), layer-cake stratigraphy is only an approximation of the pre-Neogene structure. All the NNW-SSE profiles were tested with one, two, or three basements nappe slices involved in thrusting. Within the Lombardian Basin and Trento Platform along profiles 1 and 5, the surface geology was best reproduced with two basement thrust sheets (Fig. 7c and 8c). We interpret the Mesozoic Ballino-Garda Fault (Fig. 2) to ramp down to Pre-Permian basement and connect at depth with a basement detachment (Fig. 7c). However, for the Reduced Trento Platform and Atesina Volcanic Complex along profile 6 (Fig. 9c), the surface geology was best reproduced with three basement thrust sheets. The 10-12 km depth of the lower detachment in profile 1 suggests a possible connection with the lower detachment in profile 5 and the middle detachments of profile 6, both situated at 10-12 km depth (Fig. 7, 8 and 9). A possible correlation between the bottom detachments of profiles 5 and 6 is suggested by similar detachment geometries and depths down to 15 to 20 km. Lateral jumps of a few km in detachment level (Fig. 10) are interpreted to occur along major steep Permo-Mesozoic faults. These fault jumps could be an artefact produced by the uncertainty of the fault geometries at depth within the forward modelling in Move. Such a deeper basement level is required in forward models to reproduce the structures associated with the Bassano Fault west of the Schio-Vicenza Fault.

Recently, the SWATH-D seismic network (Heit et al., 2021) provided accurate hypocenters in the study area (average vertical and horizontal resolutions of ~1.7 km and of ~0.5 km, respectively; Jozi Najafabadi et al., 2020), basically confirming existing seismicity patterns (e.g., Viganò et al., 2015). The seismicity indicates that the most frontal fault systems within the eastern Southern Alps are active (Fig. 7a, 8a and 9a). Plotted onto the cross sections, the hypocenters provided an additional independent constraint on the depth of basement fault nappes and indicate a possible blind thrust system propagating southward in profiles 1-7 (Fig. 7a, 8a and 9a), (Jozi Najafabadi et al., 2020). Note that seismicity does not necessarily delineates all active faults, as deformation may occur aseismically (Sect. 6.2) or occur along different structures than the main basement thrust. We note that some hypocenters are plotting below the modelled fault detachments (Fig. 7, 8 and 9), possibly indicating the development of an even deeper southward propagating thrust sheet (Jozi Najafabadi et al. 2020). This is in agreement with focal mechanisms of recent earthquakes indicating a thrusting regime (Petersen et al., 2021). Along profile 6 (Fig. 9), this deeper deformation may be linked with the Thiene-Bassano Fault (Galadini et al. 2005; Burrato et al., 2008) whose surface expression is the Montecchio-Precalcino Hill (Viganò et al., 2018), situated isolated in the Po Plain south of the Bassano Fault (Fig. 1). At this location, the Villaverla well (VIDEPI-database) crosses a gentle anticline fold, indicating a development in the hanging wall of a blind thrust (Viganò et al., 2018). This may introduce an additional amount of shortening to profile 6 (Fig. 9), although we do not expect this be more than ~1-2 km. In addition, no offset sediments can be observed at the Montecchio-Precalcino and therefore it is indicated as a dashed line on Fig. 9. Along profile 5 no deep blind faults have been reported in the literature, however deep seismic events (Fig. 8) suggest the presence of a blind thrust sheet.
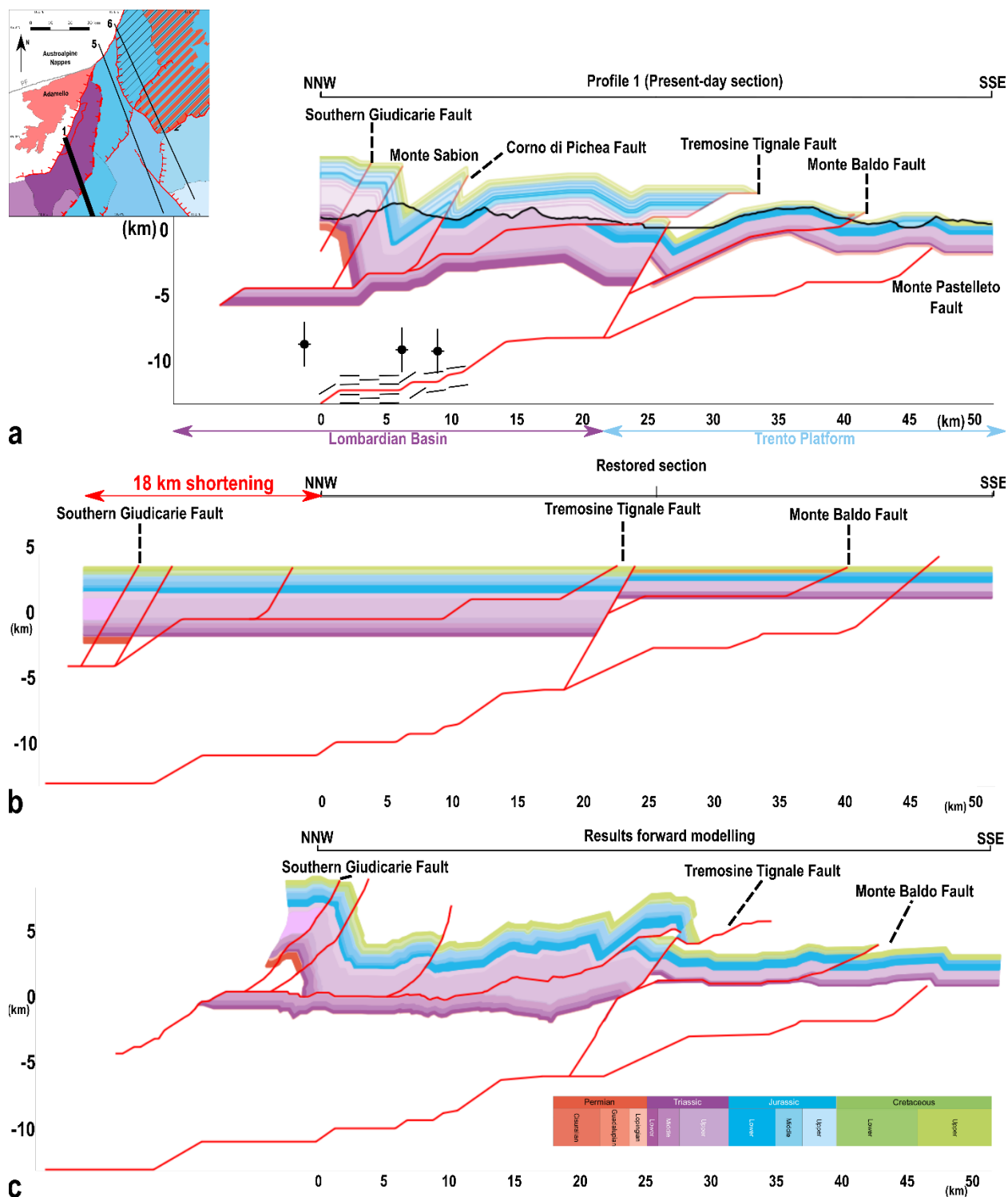
Figure 7: a) Profile 1 across the Lombardian Basin and Trento Platform; b) Profile 1 retro-deformed to a layer-cake stratigraphy; c) Results of forward modelling. Colors in legend modified after the International Chronostratigraphic Chart with pre-Permian basement beneath in white. Black dots indicate earthquake hypocenters during 2017-2018 (SWATH-D Network; Jozi Najafabadi et al., 2020; vertical bars indicate the average error range on hypocenter depths), projected from a swath covering 6 km on either side of the profile. Dashed black lines below ~10 km indicate ductile deformation.

455 **c**
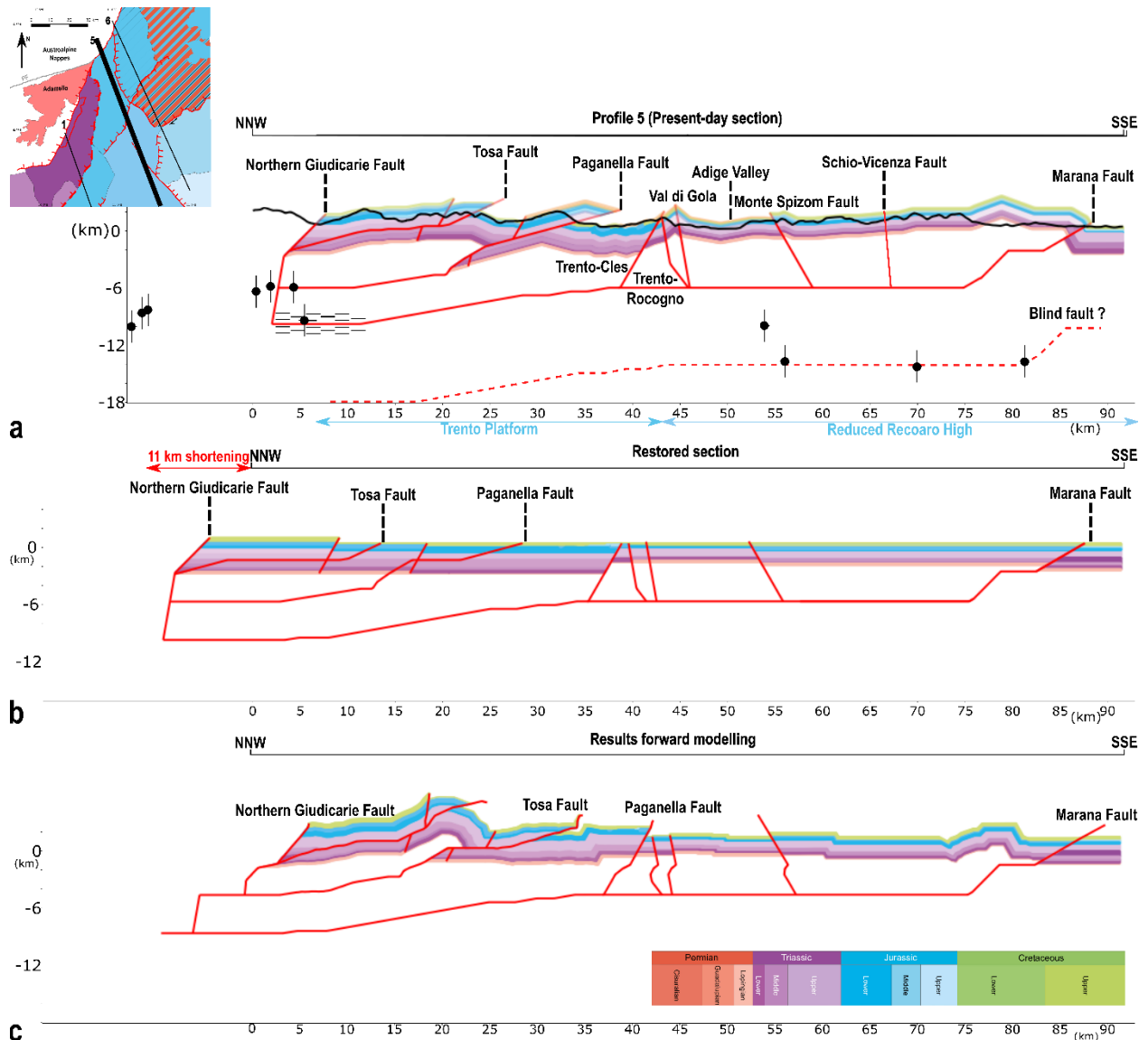
Figure 8: (a) Profile 5 across the Trento Platform and its structural Recoaro High; (b) Profile 5 retro-deformed to a layer-cake stratigraphy; (c) Results of forward modelling. Colors in legend modified after the International Chronostratigraphic Chart with pre-Permian basement beneath in white. Black dots indicate hypocenters of seismic events during 2017-2018
(SWATH-D Network; Jozi Najafabadi et al., 2020; vertical bars indicate the average error range on hypocenter depths),
460 **projected from a swath covering 6 km on either side of the profile. Dashed black lines below ~10 km indicate ductile deformation.**

465
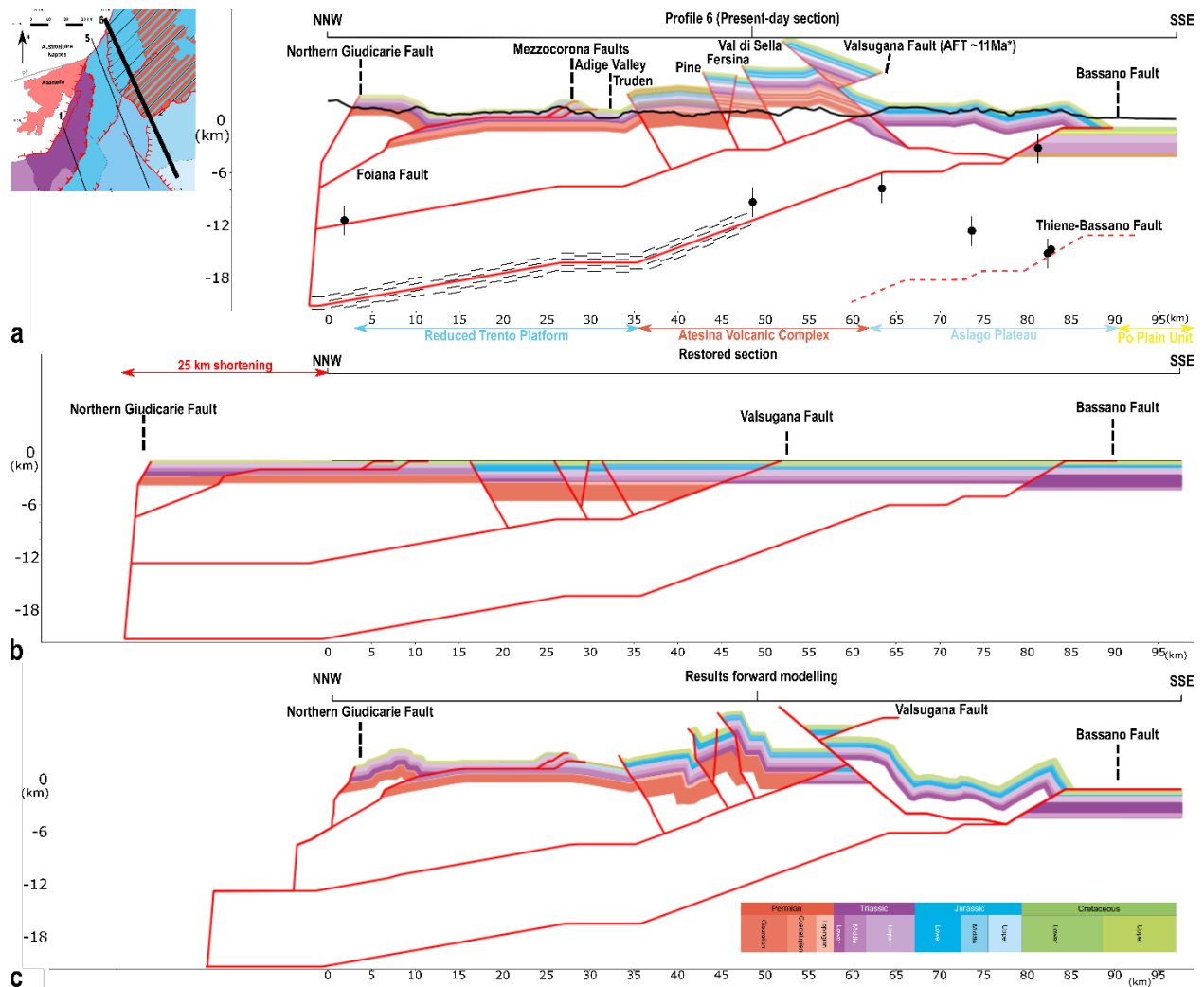
Figure 9: (a) Profile 6 across the Reduced Trento Platform, Atesina Volcanic Complex and the Asiago Plateau (AFT age for Valsugana Fault from Heberer et al. 2016; (b) Profile 6 retro-deformed to a layer-cake stratigraphy; (c) Results of forward modelling. Colors in legend modified after the International Chronostratigraphic Chart with pre-Permian basement beneath in white. Black dots indicate hypocenters of seismic events during 2017-2018 (SWATH-D Network; Jozi Najafabadi et al., 2020; vertical bars indicate the average error range on hypocenter depths), projected from a swath extending to 6 km on either side of the profile. Dashed black lines below ~10 km indicate ductile deformation.
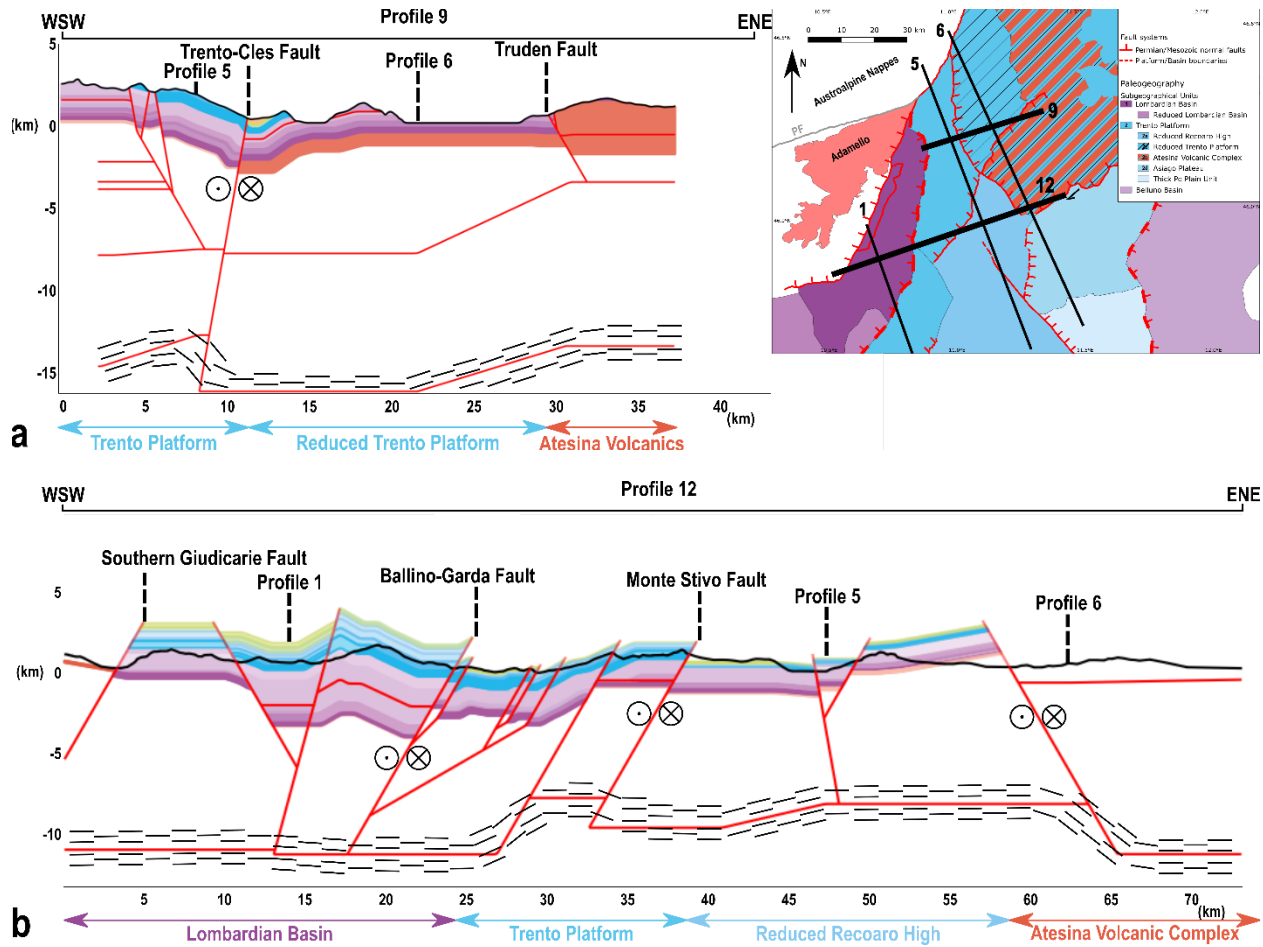
Figure 10: (a) Profile 9 across the Trento-Cles Fault separating the Trento Platform and Reduced Platform; (b) Profile 12 across the Ballino-Garda Fault between the Lombardian Basin and Trento Platform. Dashed lines at and below ~10 km indicate ductile flow.

6   Discussion

6.1   Kinematic divisions of the Giudicarie Belt

The lateral variation in shortening described above follow Permian-Mesozoic paleogeographic domains (Fig. 6), whose boundaries were reactivated as strike-slip faults during the Neogene. This is consistent with field observations along the Ballino-Garda, Schio-Vicenza and Trento-Cles faults and fault-slip analysis indicating strike-slip motion along these faults (Fig. 4). We interpret the TC-SV fault system to act as a major sinistral transfer zone (Fig. 11), accommodating the largest variation of shortening along the Giudicarie Belt (between Profiles 5 (11 km) and 6 (25 km); Fig. 6) and therefore subdividing the area into two kinematic domains (1) and (2), west and east of the TC-SV fault system, respectively (Fig. 11).

Based on age constraints (section 4), we subdivide furthermore the shortening phases along each cross section into southern (actively deforming) and northern (inactive) segments. We estimate the amount of strike-slip motion along

495   the TC-SV fault system by comparing shortening on either side of the fault (Fig. 11), which results in minimum estimates of 4 km along the SV and 9 km along the TC. Strike-slip motion along the Ballino-Garda Fault is estimated to be no more than 6 km (Picotti et al., 1995). As profile 5 straddles the SV, and profiles 3 and 4 intersect the Ballino-Garda Fault, the amount of shortening along these profiles may be underestimated by a few km, due to movement of rock volume out of the 2-D section trace.

500

The difference in shortening within the three sectors is attributable to changes in stratigraphy across these faults that are inherited from Permo-Mesozoic time. For example, in the western sector within the Lombardian Basin, most shortening is taken up by the thin-skinned Tremosine-Tignale Fault, which has a long detachment at the base of the Calcare Di Zu and consequently stacks the Dolomia Principale (Fig. 7a). The Ballino-Garda Fault is its lateral ramp

505   (Picotti et al., 1995) and therefore does not continue to the Trento Platform. The sedimentary cover is much thicker in the Lombardian Basin than in the Trento Platform (Fig. 2) and comprises a thick Jurassic sequence of slope and deep-water deposits that favor the development of extended decollements. In the Trento Platform similar stacking of the Dolomia Principale can be observed along the Tosa, Mezzocorona and Paganella Faults (Fig. 8 and 9). However, their fault displacements are much smaller, possibly due to the presence of different decollement layers within the

510   sedimentary cover.

Another example is in the eastern sector (northeast of TC-SV fault system), where most shortening is taken up by the Valsugana Fault and the inversion of a Permian graben containing the Atesina Volcanic Complex. The Calisio Fault represents the lateral ramp of the Valsugana Fault, which is connected with the Trento-Cles Fault (Fig. 1; Selli et al.,

515   1996), indicating the Valsugana Fault cannot be traced to the Trento Platform. Although the Valsugana Fault exhumes Pre-Permian basement in its hanging wall, the sedimentary cover of the Atesina Volcanic Complex is much thicker than that of the Trento Platform and contains competent volcanic and pyroclastic deposits of the Lower Permian Formazione di Ora and Formazione di Gargazzone, which are less abundant within the Trento Platform. We propose that the thick sedimentary cover of the Atesina Volcanic Complex favored a different tectonic style with a contrasting

520   amount of shortening due to the reactivation of former Permian normal faults as steep Neogene thrusts.

We argue that these local variations in shortening in the eastern Southern Alps are related to inherited paleogeographic features from Permian to Jurassic times with the majority of the deformation focused within the Lombardian Basin and the Atesina Volcanic Complex, that have a thicker sedimentary cover than the Trento Platform, which is composed

525   of mainly competent carbonate platforms. Moreover, internal fragmentation of the Adriatic indenter along the NGF and TC-SV fault system played a major role in strain partitioning (discussed in Sect. 6.2)
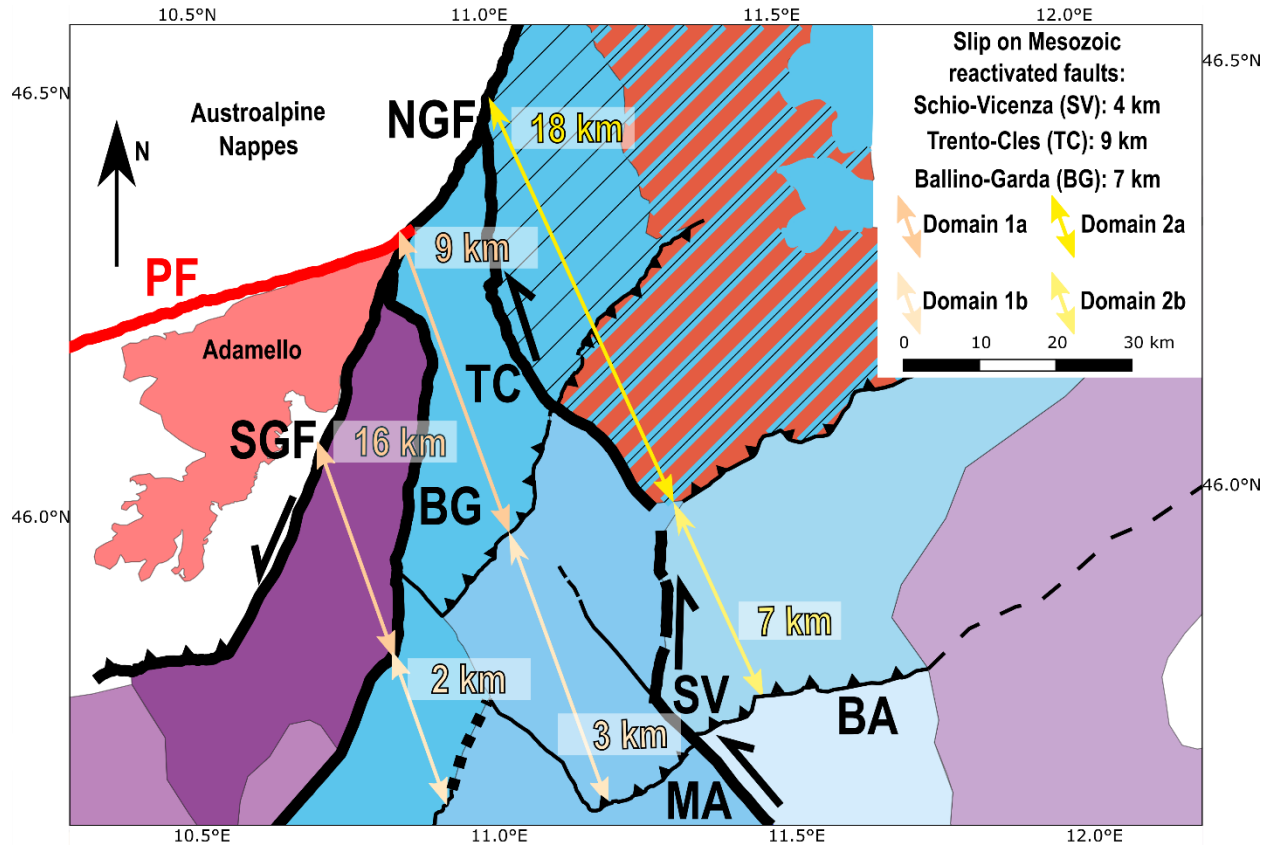
Figure 11: Lateral variation of shortening coincide with paleogeographic domains (Fig. 2), bounded by Mesozoic faults (BG, SV, TC) that were reactivated as Neogene strike-slip faults. The TC-SV fault system accommodated the largest variation of shortening and subdivides the area in two kinematic domains (1) and (2), west and east thereof, respectively. Each profile is furthermore subdivided into a northern and southern segment based on the age of deformation, with the northern domains indicating older deformation of the Giudicarie/Valsugana phase, and southern domains with a younger to active phase of shortening along the Southern Alpine orogenic front (labelled as the Marana (MA) and Bassano Faults (BA) (see Fig. 12)). See Fig. 1 for fault abbreviations.

6.2 Lateral variations in Neogene shortening across the eastern Southern Alps

The presented model of dominantly thick-skinned tectonics with three basement thrust sheets is in agreement with the cross section across the Dolomites of Schönborn (1999). However, Schönborn (1999) estimated twice the shortening in his profile across the Dolomites (> 50 km; orange line on Fig. 12). Although his cross section transects the Belluno Thrust, which is not considered in our study, the 4-5 km of displacement along this thrust (Schönborn, 1999) is insufficient to explain the difference in shortening (c. 25 km). In fact, shortening estimated by Schönborn (1999) along the Valsugana-Belluno system (22 km) is similar to our estimate of 18 km along this same system (Fig. 9). The difference between Schönborn (1999) and our study is mainly due to different interpretations of the Bassano Fault, which Schönborn associated with 33 km of shortening, while we only propose 7 km. Schönborn (1999)'s 33 km estimate is based on hinterland-dipping panels above footwall ramps, which must be matched with hanging wall geometries. Other profiles transecting the Bassano Fault published by Selli (1998) (close to the TC-SV fault system; parallel to our profile 6) and Castellarin and Cantelli (2000) (parallel to the section of Schönborn, 1999; orange section

in Fig. 12) indicate 33 and 35 km of Neogene shortening, respectively, of which 14 km and 19 km were accommodated by the Bassano Fault. Along profile 6 (Fig. 9) surface measurements of layer dips indicate that several hinterland-dipping strata of Schönborn (1999) are not observed at the surface in the hanging wall of the Bassano Fault. Therefore, we prefer the 7 km shortening estimate in our study area (Fig. 9) and the 19 km towards the east from Castellarin and Cantelli (2000), to the 33 km of Schönborn (1999).

More to the east, Nussbaum (2000) presented cross sections with several basement thrust sheets and an estimated minimum of 50 km shortening (blue line on Fig. 12). To the west of the Giudicarie Belt, Picotti et al. (1995) obtained shortening estimates of 30 to 40 km (purple line on Fig. 12). The main difference between cross sections h, g and f of Picotti et al. (1995) and cross sections 1 to 7 of this study is the major thin-skinned component of shortening beneath the Po Plain west of Lake Garda (Picotti et al., 1995; and references therein); this shortening decreases towards its lateral ramps up to the Adige Valley. Such buried thin-skinned shortening is not present further to the east, as shown by a seismic survey across the Po Plain directly east of the Schio-Vicenza Fault (Pola et al., 2014).

In addition, the TC-SV fault system seems to be the lateral boundary for most thrust systems, as thrusts merge with it and cannot be traced across. It also coincides with contrasting (though partly overlapping) ages of shortening (Fig. 11), which forms the basis for a distinction between kinematic domains 1 and 2 (Fig. 12). Kinematic domain 1 contains the Val Trompia-sector of the Giudicarie Belt with ~18 km of Late Oligocene to Early Miocene shortening along thrusts that merge with the NGF and SGF (Picotti et al., 1995; Fig. 12). The same thrusts then accommodated at least ~12-22 km of Middle Miocene to recent shortening. In kinematic domain 2, a minimum of 25 km of post-Middle Miocene shortening (Fig. 6, 9, 11 and 12) was accommodated directly east of the TC-SV fault system, broadly coeval with shortening in kinematic domain 1. Given the proximity of profile 6 to the TC-SV fault system, a major strike-slip corridor, significant out-of-plane motion along these profiles may have occurred. Therefore, we have included the estimated 35 km of Neogene shortening of Castellarin and Cantelli (2000) in the Neogene displacement vector triangle of domain 2 (Fig. 12).

We note that the shortening directions in the eastern Southern Alps shifted from NNE-SSW during the Late Oligocene to Early Miocene towards NNW-SSE during the Middle Miocene. The Late Oligocene shortening direction has been determined with mesostructural analysis and tectonic reconstructions (Castellarin et al., 1992; Picotti et al., 1995) based on field data (Schönborn, 1992; Picotti et al., 1997) and subsurface data (e.g. Fantoni and Franciosi, 2010). This shift in shortening directions is an important constraint on drawing displacement vector triangles (Fig. 12), as the hypotenuse of these should be parallel to the motion direction. Consequently, the hypotenuse of the Late Oligocene displacement triangle is oriented NNE-SSW (Fig. 12; parallel to NGF and oblique to the profile from Picotti et al., 1995), whereas the hypotenuse of the Middle Miocene displacement triangle is oriented NNW-SSE (Fig. 12; parallel to profiles 1 to 7). Using this triangular approach, we estimate 40-47 km of Late Oligocene to Middle Miocene displacement along the NGF, a calculation we discuss step by step in Sect. 6.4.
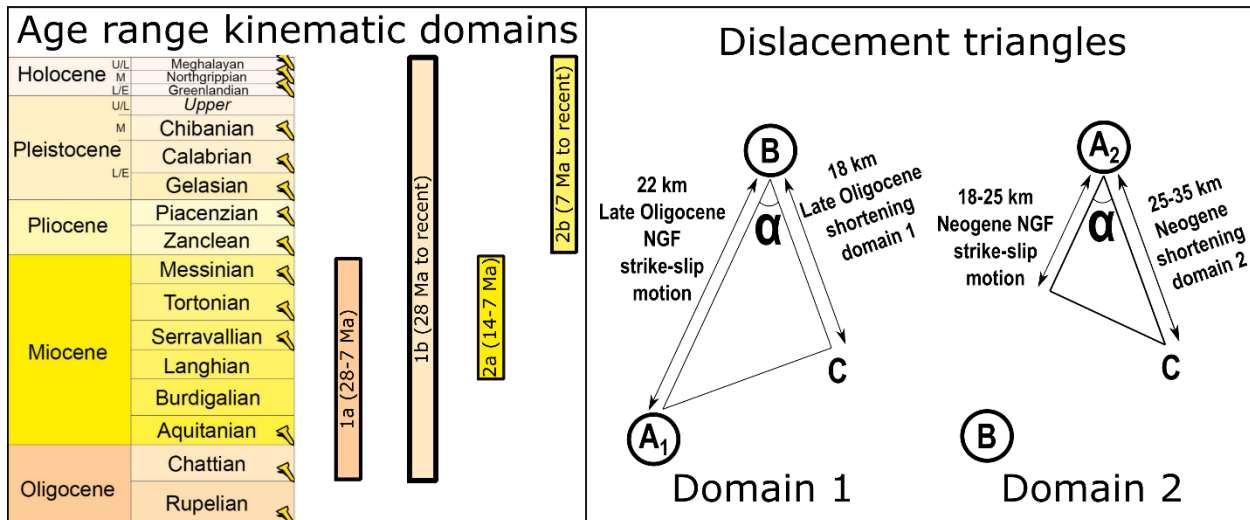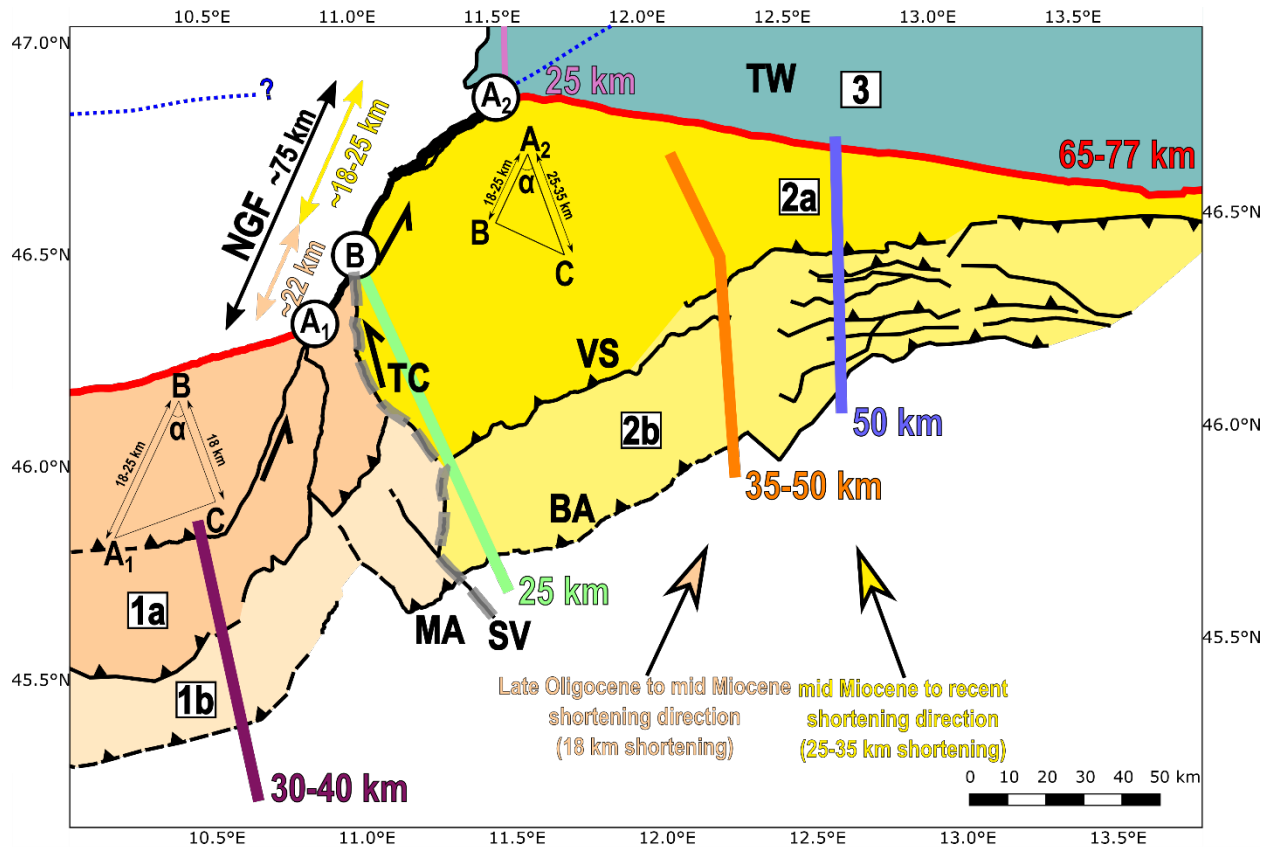
585   **Figure 12: Kinematic map of the eastern Southern Alps, divided in two domains east and west of the TC-SV fault system (dashed in grey). These made contrasting and partly overlapping kinematic contributions to sinistral strike-slip offset along the NGF. The subdivision into domains a and b is based on the age of deformation (see legend and Sect. 4). Seismicity in domains 1b and 2b indicates that shortening is still ongoing. Profile traces from this study (green), Picotti et al., (1995, purple), Schönborn (1999, orange; parallel to the cross sections of Castellarin and Cantelli, 2000), Nussbaum (2000, blue),**
590   **Favaro et al., (2017) (pink), and the inferred surface trace of a putative Adriatic crustal wedge (Gebrande et al., 2002, blue dashed) are indicated. Triangle A₁BC depicts the geometrical relationship between Late Oligocene to Early Miocene shortening in kinematic domain 1 of the Giudicarie Belt (vector BC) and motion along the NGF (vector AB), which is estimated to be ~18-25 km. This was obtained by projecting 18 km of shortening along the Val Trompia sector of the Giudicarie Belt (Picotti et al., 1995, purple). Triangle A₂BC depicts the geometrical relationship between Middle Miocene**

595 **shortening in kinematic domain 2 of the Giudicarie Belt (vector A$_2$C) and motion along the NGF (vector AB), which is estimated to be at least ~35-50 km. This was obtained by projecting 25-35 km (green) of minimum shortening across the Giudicarie Belt east of the TC-SV fault system. Fault abbreviations: BA=Bassano, MA=Marana, NGF=Northern Giudicarie Fault SV=Schio-Vicenza, VS=Valsugana**

600 Based on stratigraphic and radiometric age criteria (Sect. 4), we further divide domains 1 and 2 into sub-domains a and b (Fig. 12), with ongoing shortening in domain b indicated by seismicity. Low instrumental seismicity and high strain rates in the central part of domain 2b (Fig. 13; Serpelloni, 2016) might indicate a seismic gap (Anselmi et al., 2011). Note that strain rates are also relatively high in the Friuli area where there is a prominent cluster of seismicity (Fig. 13; see e.g. Bressan et al., 2016). This could be due to its junction with the Dinaric system, and/or an increase of

605 shortening towards the East (Nussbaum, 2000) due to counterclockwise rotation of Adria with respect to Europe (e.g. Ustaszewski et al. 2008; Le Breton et al. 2017; Mazzoli and Helman, 1994). We note that in the reconstruction of Mazzoli and Helman (1994) the relative motion vectors of Africa relative to Europe from the Late Oligocene to Middle Miocene shift from NNE-SSW to NNW-SSE, similar to the observed reorientation of shortening directions in the eastern Southern Alps (e.g. Castellarin et al, 1992). This may suggest that the shortening directions in the eastern

610 Southern Alps coincide with large-scale plate motions, a point previously made by Caputo et al. (2010).
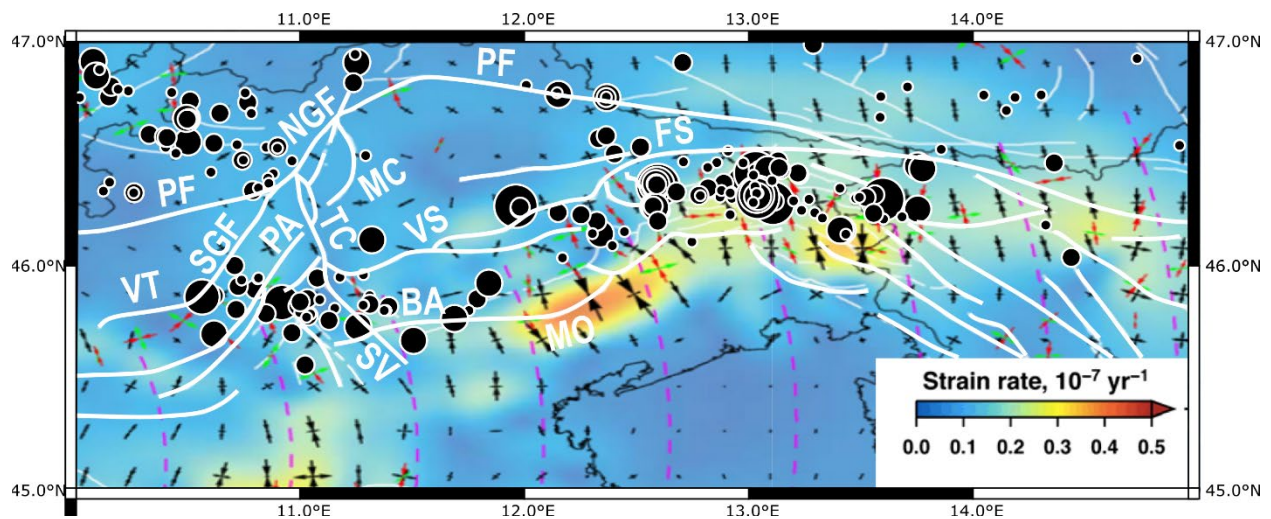
Figure 13: Epicenters of seismic events from 2017-2018 (M$_L$ ≥ 1; size of black dots indicates earthquake magnitudes up to M$_L$ 4.2) compiled from the SWATH-D Network (Jozi Najafabadi et al., 2020) superposed on strain rates determined from
615 **GPS velocities (after Serpelloni et al., 2016). Note that the area in the center with the highest strain rates (vicinity of the Montello Thrust) coincides with lower seismic activity, although clustering of low-magnitude events has been reported (Moratto et al., 2019; Romano et al., 2019). Abbr.: FS=Fella-Sava Fault; see Fig. 1 for the other fault abbreviations.**

6.3 Kinematic link between shortening along the Giudicarie Belt and sinistral motion along the NGF

620 Variations in shortening along strike of the Giudicarie Belt may be attributed to large-scale strain partitioning, especially near the TC-SV fault system (Fig. 12). This system merges with the NGF thereby transferring differential shortening between domains 1 and 2 to the NGF and contributing to the sinistral offset along the NGF (Fig. 12 and 14). Figure 14 shows a reconstruction from Late Oligocene to present and uses displacement vector triangles for

different time slices to show how shortening contributed to the observed sinistral offset along the NGF. During the Late Oligocene to Early Miocene, 18 km of shortening in domain 1 was transferred to a minimum of 22 km of motion along the NGF (see displacement vector triangles in Fig. 14). Subsequently, coeval shortening in domains 1 and 2 since the Middle Miocene contributed at least 18 to 25 km of additional motion along the NGF (Fig. 14). The range of 18 to 25 km motion along the NGF since the Middle Miocene reflects the uncertainty in minimum shortening estimates in kinematic domains 1 and 2 related to the presence or absence of putative duplexes at depth along profiles 5 and 6 (Fig. 8 and 9; see discussion in supplementary data repository, Verwater et al. 2021). Combining the estimates of 22 km of Late Oligocene to Early Miocene sinistral slip and another 18 to 25 km of Middle Miocene to recent slip on the NGF yields a total of 40 to 47 km of sinistral offset along this fault since the Late Oligocene. These minimum 40 to 47 km of Oligocene to Neogene strike-slip displacement along the NGF may be insufficient to solve the question whether the observed 75 km of sinistral displacement on the NGF is exclusively Oligocene, such that the dextral PF would acquire its interpreted straight pre-Oligocene geometry, as discussed above in Sect. 1 (Laubscher 1991; Schmid and Kissling 2000; Handy et al. 2015).

We note that some previous workers regard the NGF to have accommodated no more than 30-40 km of sinistral displacement (Picotti et al., 1995; Castellarin et al., 2006b) or even less (15 km, Viola et al., 2001), which are significantly lower than our minimum estimate for displacement on the NGF. These authors used small-scale markers and only considered motion along parts of the Giudicarie Fault System (the Passeier fault in Viola et al., 2001; the SGF in Castellarin et al., 2006b) or used slightly lower shortening estimates (Picotti et al., 1995). These studies further based their view on Mesozoic paleogeographical variations on either side of the NGF (Castellarin and Vai, 1981; Picotti et al., 1995; Prosser, 1998) that are at a low angle with the NNW-striking, early Mesozoic facies change going from the Trento Plateau to the Lombardian Basin. They interpret this near-linear coincidence as evidence for a pre-Alpine (Mesozoic) offset, thus rendering the map-view offset along the PF to be partly an artifact of Mesozoic rift tectonics. In addition, Müller et al. (2001) estimated a shortening of more than 40 km based on jumps in metamorphic grade across the NGF, which if valid, would suggest only ~40 km of Paleogene dextral motion along the PF and allow a pre-Oligocene offset of the NGF. However, this is incompatible with the interpreted late Paleogene dextral motion on the PF of some 100-150 km (Laubscher 1991, Schmid and Kissling 2000), which would have been accommodated by a roughly equivalent amount of the late Paleogene E-W shortening at high angles to the NGF. E-W shortening of such magnitude along the NGF has not been observed.

655
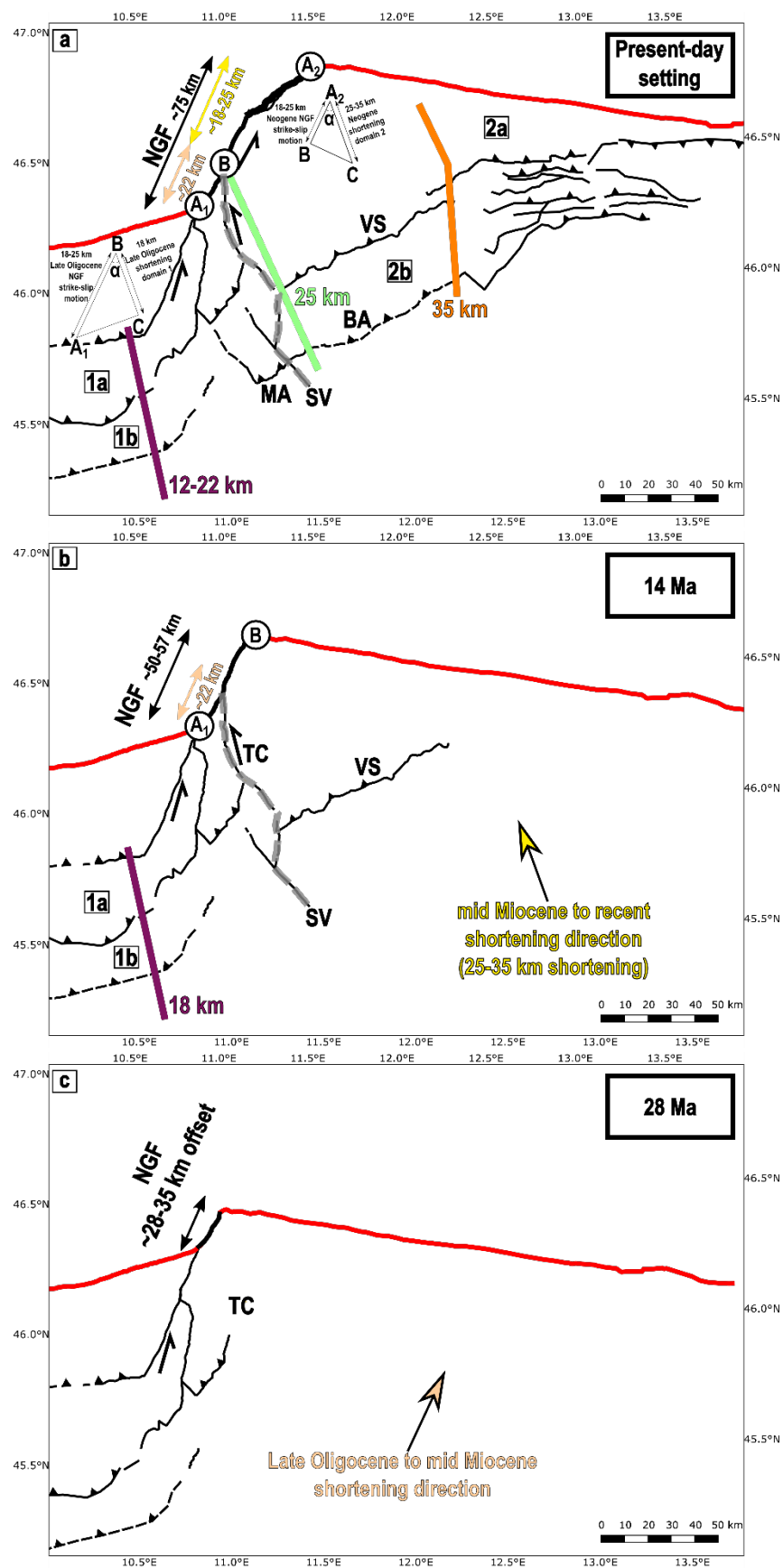
Figure 14 (previous page): Kinematic evolution of the eastern Southern Alps from the present day (a) to Late Oligocene time (c): (a) Present configuration of the eastern Southern Alps with ~75 km sinistral offset of the PF along the NGF. There are two kinematic contributions to the ~75 km of strike-slip motion: (1) 25-35 km of Middle Miocene NNW-SSE shortening across kinematic domain 1 and 2 (Fig. 12), which when projected onto the NGF, corresponds to ~18-25 km of sinistral strike-slip (displacement vector triangle A$_2$BC); (2) 18 km of Chattian to Middle Miocene, NNE-SSW to NNW-SSE shortening west of the TC-SV fault system, which when projected onto the NGF corresponds to ~22 km of sinistral strike-slip (see discussion in Sect. 3); (b) At ~14 Ma the NGF sinistrally displaced the PF by ~50-57 km (both minimum values). Since the Middle Miocene (≥14 Ma), ~20-35 km of shortening both east and west of the TC-SV fault system were transferred to motion along the NGF at ≥ 14 Ma which is therefore at this time only displaced by 50-57 km. The minimum ~50-57 km offset along the NGF at ~14 Ma is partly attributable to a minimum 18 km of Late Oligocene to Middle Miocene shortening along the Val Trompia-Giudicarie Belt ('kinematic step 1' of Picotti et al., 1995); (c) At ~28 Ma the Periadriatic Fault was only modest offset (~28-35 km). If one assumes a mean value within this range of offsets, the PF restores to a relatively straight fault showing only a minor bend north of the Adamello batholith.

6.4 Transfer of motion along the NGF to the Eastern Alps

The minimum 40 to 47 km of sinistral motion on the NGF must have been transferred into the Alpine orogenic lithosphere north of the Pustertal-Gailtal part of the PF and south of the Northern Calcareous Alps. The northern Alpine Front is not offset by an equivalent amount. Therefore, obvious structures to accommodate this displacement are in the Tauern Window, as already proposed by numerous authors (e.g., Laubscher 1991, Frisch et al. 1998, Linzer et al. 2002, Scharf et al. 2013). Based on 2-D map view kinematic reconstructions, Favaro et al. (2017) estimated at least 25 km of N-S Neogene shortening (Fig. 12) associated with km-scale upright, post-nappe folding in the Western Tauern Window, located just north of the angular junction of the NGF and PF defining the tip of the eastern Adriatic indenter. This implies that a remaining amount of N-S shortening was transferred into orogen-parallel, lateral escape of the Eastern Alps towards the Pannonian Basin (Ratschbacher et al., 1989; Frisch et al., 1998; 2000; Linzer et al., 2002; Rosenberg et al., 2007 Scharf et al., 2013; Handy et al., 2015). Estimates of lateral extrusion vary between 65-77 km (Favaro et al., 2017) and 160 km (Frisch et al., 2000). The latter amount is probably an overestimate because the authors assumed that Austroalpine units exposed at the western and eastern ends of the Tauern Window were in contact prior to Neogene extension, effectively neglecting the contribution of km-scale post-nappe upright folding to denudation (see discussion in Favaro et al. 2017). The amount of eastward motion can be roughly estimated by balancing the amount of shortening within the Southern Alps with shortening within the Tauern Window, although the amount of lateral escape as a function of indentation also depends on the depth of detachment underneath the Tauern Window, which is unknown. Our minimum estimates for Middle Miocene to recent NNW-SSE shortening within the Giudicarie Belt (~25 km) combined with Late Oligocene to Early Miocene NNE-SSW shortening estimates across the Val-Trompia fold-and-thrust belt (Picotti et al., 1995) would suggest less lateral extrusion than the 160 km proposed by Frisch et al. (2000). We therefore favor the estimate of 65 to 77 km (Favaro et al., 2017) of E-W directed, orogen-parallel extension of the Eastern Alps since 21 Ma (Favaro et al., 2017). Assuming that 40 to 47 km motion along the NGF was transferred to the Tauern Window (Laubscher, 1990) and resulted in 25 km N-S shortening in the Tauern Window (Favaro et al., 2017), a total of 65 to 72 km N-S Neogene Alpine shortening can be estimated. This range of shortening estimates is clearly less than Adria-Europe Neogene plate convergence proposed in plate tectonic reconstructions (~100 km, Van Hinsbergen et al., 2020; ~135 km, Le Breton et al., 2017, 2021). This either suggests

that the plate tectonic reconstructions are overestimating the Neogene Adria-Europe plate convergence, or alternatively, additional sources of shortening may have contributed to the overall plate convergence. This discrepancy could be attributed to three possible factors: (1) alternative interpretations of profiles across the Giudicarie Belt (see discussion in Sect. 5.1 and 5.2); (2) 'buried' shortening underneath the Po Plain (see discussion in Sect. 5.3); (3) additional N-S shortening associated with upright folding and lateral extrusion rooting in the Tauern Window, possibly associated with an Adriatic crustal wedge, as we discuss in Sect. 6.5 below.

6.5   Transfer of motion at lower crustal – mantle depths

The contribution of shortening along the Giudicarie Belt to offset along the NGF requires that the basal detachment of the former roots in the latter. Alternatively, the basal detachment of the Giudicarie Belt and NGF occupy different depths, implying the absence of a kinematic link between shortening along the Giudicarie Belt and motion along the NGF. Additional shortening could be accommodated by a lower crustal Adriatic wedge, which according to reflection seismic studies extends 25 km north of the PF beneath the Tauern Window (Fig. 12; Gebrande et al., 2002; Lüschen et al., 2004; Castellarin et al., 2006a). This would necessitate decoupling between relatively weak orogenic crust and rigid denser lower Adriatic crust. The shortening associated with this sub-Tauern wedge can be no more than its 25 km length measured in a N-S direction, which is equal or less than the minimum amount of N-S shortening in our sections and along other transects of the eastern Southern Alps (Schönborn 1999; Castellarin and Cantelli 2000, Nussbaum 2000). Our results show that along-strike variations in Neogene shortening within the Giudicarie Belt coincide with pre-existing structures, indicating a main detachment horizon exists beneath the Giudicarie Belt. This detachment horizon could either be linked at depth with the NGF, PF and a lower crustal Adriatic wedge underneath the Eastern Alps (sub-Tauern wedge; Lüschen et al., 2004; Castellarin et al., 2006a) or alternatively could extend northwestward of the NGF and linked with the Adriatic lower crustal wedge beneath the central Alps. We consider the latter hypothesis to be rather unlikely given the wide E-W extent of this wedge towards the Western Alps and the modest amount of shortening along the Giudicarie Belt. The Eastern Alpine crustal wedge may be shorter than the lower crustal Adriatic wedge in the Central Alps (Schmid et al. 1996; Rosenberg and Kissling, 2013). Nevertheless, its relationship with Neogene shortening across the eastern Southern Alps remains enigmatic. Possibly, the amount of shortening observed at the surface and within the Adriatic crust is an expression of lateral variations in the strength of the Adriatic upper and lower crust, as also proposed for the Central Alpine lower crustal Adriatic wedge (Rosenberg and Kissling, 2013). To test this hypothesis, future studies using local earthquake tomography are necessary to image and delineate a potential lower Adriatic crustal wedge beneath the Tauern Window and Eastern Alps. Such studies may also constrain the dip of the NGF at depth, which in existing Moho maps does not appear to offset the Moho (e.g., Spada et al. 2013).

Previous studies have also suggested the presence of an Adriatic slab underneath the Eastern Alps (Lippitsch et al., 2003; Handy et al., 2015). Recent seismic tomography studies using the dense AlpArray seismic network indicate however that the slab beneath the Eastern Alps is completely detached from the orogenic crust and extends down to, and locally beyond, the 410 km discontinuity marking the top of the mantle transition zone (Handy et al., 2021). This

slab length is far greater than the 25-50 km estimates of shortening in the eastern Southern Alps (this study and Schönborn 1999), which represent accreted units of the Adriatic plate. This discrepancy strongly favors a European origin of the slab and effectively rules out an Adriatic origin as proposed in earlier studies (e.g., Lippitsch et al. 2003, Handy et al. 2015).

740 **7   Conclusion**

This study focuses on constraining its Neogene kinematics and depth of deformation, in particular the kinematic link between shortening in the Giudicarie Belt and motion along the NGF, and their connection to deeper structures. Fault-slip analysis confirms that the main Neogene shortening direction is NNW-SSE. Balancing of 7 geological cross sections within the Giudicarie Belt indicates a dominant thick-skinned structural style of deformation, as shown by

745 ramp anticlines exposing Pre-Permian basement in the hanging wall of faults and clustering of recent seismicity at ca. 15 to 20 km depth within the basement. This thick-skinned tectonic implies a modest amount of shortening (8-25 km) within the studied area. The variations in Neogene shortening coincide with major Permian-Mesozoic paleogeographic domains that divide the studied area into two kinematic domains, west and east of the Trento-Cles – Schio-Vicenza transfer fault system that accommodated about 13 km of sinistral slip. The lateral variation in shortening reflects

750 competence contrasts and sedimentary thickness variations across the paleogeographic domains. Domains of thickest sedimentary cover, comprising relatively incompetent slope deposits, has accommodated more Neogene shortening (17-25 km), whereas domains of thinnest sedimentary cover, with competent platform carbonates, accommodated the least amount of shortening (8-12 km).

755 Projecting the amount of shortening onto the NGF yields a minimum of 40 to 47 km of sinistral slip along this fault since the Late Oligocene. This amount may be insufficient to fully explain the 75 km of sinistral offset of the Periadriatic Fault, although a possible additional source of Neogene shortening could be a potential Adriatic lower crustal wedge. Future work using local earthquake tomography is necessary to test this hypothesis and determine its potential lateral extent and relationship to shortening within the upper crust. Here, we follow the interpretation that

760 Adriatic indentation into the Eastern Alps is responsible for most of the 75 km sinistral offset along the NGF, triggering lateral escape of the Eastern Alps. Furthermore, we interpret the eastward increase of shortening, from 11 km to 25 km, within our study area to reflect lateral variations in strength of the Adriatic indenter due to inherited Permian to Mesozoic tectonic structures and paleogeographic domains.

Data Availability

765 All reconstruction and forward modelling files, as well as the complete set of cross sections of this study are available in the following data repository website:

https://dataservices.gfz-potsdam.de/panmetaworks/review/3c9729f2be33ab6678f45a7f3e2a7f21ccbac9a79a5859eda9d0351907fdf8c5/

Author contribution

The project was conceived by MH, ELB and CH as part of the German Research Priority Program (SPP-2017) "Mountain Building in 4-Dimensions, an interdisciplinary arm of the European *AlpArray* Project. Fieldwork, fault-slip analysis, drawing of stratigraphic columns, construction and balancing of cross sections were performed by VF under the supervision of ELB, MH and with the advice of VP. VF wrote the manuscript with major contributions from ELB and MH. AJN and CH provided the earthquake catalogue and participated in the discussion on seismicity and active structural domains of the Southern Alps.

Competing interests

The authors declare that they have no conflict of interest.

Acknowledgment

We acknowledge financial support of the German Science Foundation (DGF; BR 4900/3-1, HA 2403/22-1 and HA 3326/5-1). We would like to thank Petex for granting the FU Berlin educational licenses of the MOVE suite. This work greatly beneficiated from stimulating conversations with Philipp Balling, Jan Pleuger, Philip Groß and Julian Hülscher, as well as a visit in the field with Alfio Viganò (ICAMO-Trento) and discussions with Giuliana Rossi, Alessandro Vuan and Stefano Parolai at the OGS in Trieste.

References

Anderlini, L., Serpelloni, E., Tolomei, C., De Martini, P. M., Pezzo, G., Gualandi, A., and Spada, G.: New insights into active tectonics and seismogenic potential of the Italian Southern Alps from vertical geodetic velocities, Solid Earth, 11, 1681–1698, https://doi.org/10.5194/se-11-1681-2020, 2020.

Anselmi, M, Govoni, A., De Gori, P. and Chiarabba, C.: Seismicity and velocity structures along the south-Alpine thrust front of the Venetian Alps (NE-Italy), Tectonophysics, 513, 37 – 48, doi: 10.1016/j.tecto.2011.09.023, 2011.

Avanzini, M., Bargossi, G., Borsato, A. and Selli, L.: Note illustrative della Carta Geologico d'Italia alla scala 1:50000. Foglio 060, Trento, Provincia Autonoma di Trento, Provincia Autonoma di Bolzano, Roma, 2010.

Bartolomei, G., Corsi, M., Dal Cin, R., D'Amico, C., Gatto, G., Gatto, P., Nardin, M., Rossi, D., Sacerdotti, M. and Semenza, E.: Note illustrative della Carta Geologico d'Italia. Foglio 21, Trento, Serv. Geol. d'Italia, Roma, 1969.

Bernoulli, D. and Jenkyns, H.: Alpine, Mediterranean and Central Atlantic Mesozoic Facies in Relation to the Early Evolution of the Tethys, doi: 10.2110/pec.74.19.0129, 1974.

Bernoulli, D. and Winkler, W.: Heavy mineral assemblages from Upper Cretaceous South- and Austroalpine flysch sequences (northern Italy and southern Switzerland): source terranes and palaeotectonic implications, Eclogae Geologicae Helvetiae, 83, 287-310, 1990.

805

Bertotti, G., Picotti, V., Bernoulli, D. and Castellarin, A.: From rifting to drifting: tectonic evolution of the South-Alpine upper crust from the Triassic to the Early Cretaceous, Sedimentary Geology, 86, 53-76, doi: 10.1016/0037-0738(93)90133-P, 1993.

810   Bosellini, A., Carraro, F., Corsi, M., De Vechi, G., Gatto, G., Malaroda, R., Sturani, C., Ungaro, S and Zanettin, B.: Note illustrative della Carta Geologico d'Italia. Foglio 49, Verona, Serv. Geol. d'Italia, Roma, 1969.

Boyer, S.: Styles of folding within thrust sheets: examples from the Appalachian and Rocky Mountains of the U.S.A. and Canada, Journal of Structural Geology, 8, 325-339, doi: 10.1016/0191-8141(86)90053-2, 1986.

815

Brack, P.: Structures in the Southwestern Border of the Adamello Intrusion (Alpi Bresciane, Italy), Schweizerische mineralogische und petrographische Mitteilungen, 61, 37-50, 1981.

Braga, G., Gatto, G., Gatto, P., Gregnanin, A., Massari, F., Medizza, F. and Semenza, E.: Note illustrative della Carta
820   Geologico d'Italia, Foglio 22, Feltre, Serv. Geol. d'Italia, Roma, 1971.

Bressan, G., Ponton, M., Rossi, G., and Urban, S.: Spatial organization of seismicity and fracture pattern in NE Italy and W Slovenia, Journal of Seismology, 20, 511–534, 2016.

825   Burrato, P., Poli, M., Vannoli, P., Zanferrari, A., Basili, R., and Galadini, F.: Sources of Mw 5+ earthquakes in northeastern Italy and western Slovenia: An updated view based on geological and seismological evidence, Tectonophysics, 453, 157-176, doi: 10.1016/j.tecto.2007.07.009, 2008.

Caputo, R., Poli, M. and Zanferrari, A.: Neogene–Quaternary tectonic stratigraphy of the eastern Southern Alps, NE
830   Italy, Journal of Structural Geology, 32, doi: 1009-1027. 10.1016/j.jsg.2010.06.004, 2010.

Castellarin, A. and Cantelli, L.: Neo-Alpine evolution of the Southern Eastern Alps, Journal of Geodynamics, 30, 251-274, doi: 10.1016/S0264-3707(99)00036-8, 2000.

835   Castellarin, A. and Vai, G.: Importance of Hercynian tectonics within the framework of the Southern Alps, Journal of Structural Geology, 3, 477-486, doi: 10.1016/0191-8141(81)90047-X, 1981.

Castellarin, A., Braga, G., Corsi, M., De Vecchi, G., Gatto. G., Gatto, G., Largaiolli, T., Monese, A., Mozzi, G., Rui, A., Sassi, F. and Zirpoli, G.: Note illustrative della Carta Geologico d'Italia, Foglio 36, Schio, Serv. Geol. d'Italia, Roma, 1968.

Castellarin, A., Cantelli, L., Fesce, A., Mercier, J., Picotti, V., Pini, G., Prosser, G. and Selli, L.: Alpine compressional tectonics in the southern Alps: relationships with the N-Apennines, Annales Tectonicae, 6, 62-94, 1992.

Castellarin, A., Picotti, V., Cantelli, L., Claps, M., Trombetta, L., Selli, L., Carton, A., Borsato, A., Daminato, F., Nardin, M., Santuliana, E., Veronese, L. and Bollettinari, G.: Note illustrative della Carta Geologico d'Italia alla scala 1:50000, Foglio 080, Riva Del Garda, Provincia Autonoma di Trento, L.A.C., Firenze, 2005.

Castellarin, A., Nicolich, R., Fantoni, R., Cantelli, L., Sella, M. and Selli, L.: Structure of the lithosphere beneath the Eastern Alps (southern sector of the TRANSALP transect), Tectonophysics, 414, 259-282, doi: 10.1016/j.tecto.2005.10.013, 2006a.

Castellarin, A., Vai, G. and Cantelli, L.: The Alpine evolution of the Southern Alps around the Giudicarie faults: A Late Cretaceous to Early Eocene transfer zone, Tectonophysics, 414, 203-223, doi: 10.1016/j.tecto.2005.10.019, 2006b.

Dal Piaz, G.: Sull'esistenza del Pliocene marino nel Veneto: Accademia Scientifica Veneto Istriana, Atti, 5, 1912.

Dal Piaz, G., Castellarin, A., Martin, S., Selli, L., Carton, A., Pellegrini, G., Casolari, E., Daminato, F., Montresor, L., Picotti, V., Prosser, G., Santuliana, E. and Cantelli, L.: Note illustrative della Carta Geologica d'Italia alla scala 1:50.000, Foglio 042 Malè, 2007.

Delvaux, D. and Sperner, B.: Stress tensor inversion from fault kinematic indicators and focal mechanism data: the TENSOR program, Geological Society, London, Special Publications, 212, 75-100, 2003.

Dewey, J., Helman, M., Knott, S., Turco, E. and Hutton, D.: Kinematics of the western Mediterranean, Geological Society, London, Special Publications, 45, 265-283, doi: 10.1144/GSL.SP.1989.045.01.15, 1989.

Doglioni, C.: Thrust tectonics examples from the Venetian Alps, Studi Geol. Camerti, 117-129, 1990.

Doglioni, C.: The Venetian Alps thrust belt, doi: 10.1007/978-94-011-3066-0_29, 1992.

Doglioni, C. and Bosellini, A.: Eoalpine and Mesoalpine tectonics in the Southern Alps, Geologische Rundschau, 76, doi: 10.1007/BF01821061, 1987.

875

Fantoni, R. and Franciosi, R.: Tectono-sedimentary setting of the Po Plain and Adriatic Foreland, Rendiconti Lincei-scienze Fisiche E Naturali, 21, 197-209, doi: 10.1007/s12210-010-0102-4, 2010.

Favaro, S., Schuster, R., Handy, M., Scharf, A. and Pestal, G.: Transition from orogen-perpendicular to orogen-parallel
880   exhumation and cooling during crustal indentation — Key constraints from 147Sm/144Nd and 87Rb/87Sr geochronology (Tauern Window, Alps), Tectonophysics, 665, 1-16, doi: 10.1016/j.tecto.2015.08.037, 2015.

Favaro, S., Handy, M., Scharf, A. and Schuster, R.: Changing patterns of exhumation and denudation in front of an advancing crustal indenter, Tauern Window (Eastern Alps), Tectonics, 36, doi: 10.1002/2016TC004448, 2017.
885

Fondriest, M., Smith, S., Di Toro, G., Zampieri, D. and Mittempergher, S.: Fault zone structure and seismic slip localization in dolostones, an example from the Southern Alps, Italy, Journal of Structural Geology, 45, 52-67, doi: 10.1016/j.jsg.2012.06.014, 2012.

890   Franceschi, M., Massironi, M., Franceschi, P. and Picotti, V.: Spatial analysis of thickness variability applied to an Early Jurassic carbonate platform in the central Southern Alps (Italy): a tool to unravel syn-sedimentary faulting, Terra Nova, 26, doi: 10.1111/ter.12092, 2014.

Frisch, W., Kuhlemann, J., Dunkl, I. and Brügel, A.: Palinspastic reconstruction and topographic evolution of the
895   Eastern Alps during Late Tertiary tectonic extrusion, Tectonophysics, 297, 1-15, doi: 10.1016/S0040-1951(98)00160-7., 1998.

Frisch, W., Dunkl, I. and Kuhlemann, J.: Post-collisional orogen-parallel large-scale extension in the Eastern Alps, Tectonophysics, 327, 239-265, doi: 10.1016/S0040-1951(00)00204-3, 2000.
900

Fügenschuh, B., Seward, D. and Mancktelow, N.: Exhumation in a convergent orogen: The western Tauern window, Terra Nova, 9, 213 – 217, doi: 10.1111/j.1365-3121.1997.tb00015.x, 1997.

Fügenschuh, B., Mancktelow, N. and Schmid, S.: Comment on Rosenberg and Garcia: Estimating displacement along
905   the Brenner Fault and orogen-parallel extension in the Eastern Alps, Int J Earth Sci (Geol Rundsch) (2011) 100:1129–1145, International Journal of Earth Sciences, 101, doi: 10.1007/s00531-011-0725-4, 2012.

Galadini, F., Poli, M. and Zanferrari, A.: Seismogenic sources potentially responsible for earthquakes with M >= 6 in the eastern Southern Alps (Thiene-Udine sector, NE Italy), Geophysical Journal International, 161, 739-762, doi:
910   10.1111/j.1365-246X.2005.02571.x, 2005.

Gebrande, H., Luschen, E., Bopp, M., Bleibinhaus, F., Lammerer, B., Oncken, O., Stiller, M., Kummerow, J., Kind, R., Millahn, K., Grassl, H., Neubauer, F., Bertelli, L., Borrini, D., Fantoni, R., Pessina, C., Sella, M., Castellarin, A., Nicolich, R. and Bernabini, M.: First deep seismic images of the Eastern Alps reveal giant crustal wedges and transcrustal ramps, Geophysical Research Letters, 29, 92.1-92.4, doi: 10.1029/2002GL014911, 2002.

Handy, M.: The structure, age and kinematics of the Pogallo fault zone, southern Alps, northwestern Italy, Eclogae Geol. Helv., 80, 593-632, 1987.

Handy, M. and Zingg, A.: The tectonic and rheological evolution of an attenuated cross section of the continental crust: Ivrea crustal section, southern Alps, northwestern Italy and southern Switzerland, Geological Society of America Bulletin, 103, 236-253, doi: 10.1130/0016-7606(1991)103<0236:TTAREO>2.3.CO;2, 1991.

Handy, M., Babist, J., Wagner, R., Rosenberg, C. and Konrad-Schmolke, M.: Decoupling and its relation to strain partitioning in continental lithosphere: Insight from the Periadriatic fault system (European Alps), Geological Society, London, Special Publications, 243, 249-276, doi: 10.1144/GSL.SP.2005.243.01.17, 2005.

Handy, M., Schmid, S., Bousquet, R., Kissling, E. and Bernoulli, D.: Recoiling plate-tectonic reconstructions of Alpine Tethys with the geological-geophysical record of spreading and subduction in the Alps, Earth-Science Reviews, 102, 121-158, doi: 10.1016/j.earscirev.2010.06.002, 2010.

Handy, M., Ustaszewski, K. and Kissling, E.: Reconstructing the Alps–Carpathians–Dinarides as a key to understanding switches in subduction polarity, slab gaps and surface motion, International Journal of Earth Sciences, doi: 10.1007/s00531-014-1060-3, 2015.

Handy, M., Schmid, S., Paffrath, M., Friederich, W. and the AlpArray working group: European tectosphere and slabs beneath the greater Alpine area - Interpretation of mantle structure in the Alps-Apennines-Pannonian region from teleseismic Vp studies, Solid Earth Discuss., in review, 2021.

Heberer, B., Reverman, R., Fellin, M., Neubauer, F., Dunkl, I., Zattin, M., Seward, D., Genser, J. and Brack, P.: Postcollisional cooling history of the Eastern and Southern Alps and its linkage to Adria indentation, International Journal of Earth Sciences, 106, doi: 10.1007/s00531-016-1367-3, 2016.

Heit, B., Cristiano, L., Haberland, C., Tilmann, F., Pesaresi, D., Jia, Y., Hausmann, H., Hemmleb, S., Haxter, M., Zieke, T., Jaeckl, K.-H., Schloemer, A., and Weber, M.: The Swath-D network in the Eastern Alps, Seismological Research Letters, 92, doi: 10.1785/0220200377., 2021.

Hülscher, J., Sobel, E., Verwater, V., Groß, P., Chew, D. and Bernhardt, A.: Detrital apatite geochemistry and thermochronology from the Oligocene/Miocene Alpine foreland record the early exhumation of the Tauern Window, Basin Research, in review, 2021.

950

Jozi Najafabadi, A., Haberland, C., Ryberg, T., Verwater, V., Le Breton, E., Handy, M. R., Weber, M., and the AlpArray working group: Relocation of earthquakes in the Southern and Eastern Alps (Austria, Italy) recorded by the dense, temporary SWATH–D network using a Markov chain Monte Carlo inversion, Solid Earth Discuss., https://doi.org/10.5194/se-2020-192, in review, 2020.

955

Karousová, H., Plomerova, J. and Vecsey, L.: Seismic tomography of the upper mantle beneath the north-eastern Bohemian Massif (central Europe), Tectonophysics, s 564–565, 1–11, doi: 10.1016/j.tecto.2012.06.031, 2012.

960

Kästle, E., Rosenberg, C., Boschi, L., Bellahsen, N., Meier, T. and El-Sharkawy, A.: Slab break-offs in the Alpine subduction zone (Open Access), International Journal of Earth Sciences, doi: 10.1007/s00531-020-01821-z., 2020.

Keim, L. and Stingl, V.: Lithostratigraphy and facies architecture of the Oligocene conglomerates at Monte Parei (Fanes, Dolomites, Italy), Rivista Italiana di Paleontologia e Stratigrafia, 106, 123-132, doi: 10.13130/2039-4942/5393, 2000.

965

Laubscher, H.: The problem of the deep structure of the Southern Alps: 3-D material balance considerations and regional consequences, Tectonophysics, 176, doi: 103-121. 10.1016/0040-1951(90)90261-6, 1990.

970

Laubscher, H.: The arc of the Western Alps today, Eclogae Geologicae Helvetiae, 84, 631-659, 1991.

Le Breton, E., Handy, M., Molli, G. And Ustaszewski, K.: Post-20 Ma motion of the Adriatic plate - new constraints from surrounding orogens and implications for crust-mantle decoupling: Post-20 Ma motion of the Adriatic plate, Tectonics, doi: 10.1002/2016TC004443, 2017.

975

Le Breton, E., Brune, S., Ustaszewski, K., Zahirovic, S., Seton, M., and Müller, R. D.: Kinematics and extent of the Piemont–Liguria Basin – implications for subduction processes in the Alps, Solid Earth, 12, 885–913, https://doi.org/10.5194/se-12-885-2021, 2021.

980

Linzer, H., Decker, K., Peresson, H., Dellmour, R. and Frisch, W.: Balancing lateral orogenic float of the Eastern Alps, Tectonophysics, 354, 211-237, doi: 10.1016/S0040-1951(02)00337-2, 2002.

Lippitsch, R., Kissling, E. and Ansorge, J.: Upper mantle structure beneath the Alpine orogen from high-resolution teleseismic tomography, Journal of Geophysical Research, 108, doi: 10.1029/2002JB002016, 2003.

985

Luciani, V. and Silvestrini, A.: Planktonic foraminiferal biostratigraphy and paleoclimatology of the Oligocene/Miocene transition from the Monte Brione Formation (Northern Italy, Lake Garda), Mem. Sci. Geol., 48, 155-169, 1996.

990   Lüschen, E., Lammerer, B., Gebrande, H., Millahn, K. And Nicolich, R.: Orogenic structure of the Eastern Alps, Europe, from TRANSALP deep seismic reflection profiling, Tectonophysics, 388, 85-102, doi: 10.1016/j.tecto.2004.07.024, 2004.

Marrett, R. and Allmendinger, R.: Kinematic analysis of fault-slip data. Journal of Structural Geology, 12, 973-986,
995   doi: 10.1016/0191-8141(90)90093-E, 1990.

Martin, S., Bigazzi, G., Zattin, M., Viola, G. and Balestrieri, M.: Neogene kinematics of the Giudicarie fault (Central-Eastern Alps, Italy): New apatite fission-track data, Terra Nova, 10, 217 – 221, doi: 10.1046/j.1365-3121.1998.00119.x, 1998.

1000

Massari, F., Grandesso, P., Stefani, C., and Jobstraibizer, P.: A Small Polyhistory Foreland Basin Evolving in a Context of Oblique Convergence: The Venetian Basin (Chattian to Recent, Southern Alps, Italy), Spec. Publs. int. Ass. Sedim., 8, 141-168, 1986.

1005   Mazzoli, S. and Helman, M.: Neogene patterns of relative plate motion for Africa-Europe: some implications for recent central Mediterranean tectonics, Geologische Rundschau, 83, 464-468, doi: 10.1007/BF00210558, 1994.

Mitterbauer, U., Behm, M., Brückl, E., Lippitsch, R., Guterch, A., Keller, R., Koslovskaya, E., Rumpfhuber, E. and Šumanovac, F.: Shape and origin of the East-Alpine slab constrained by the ALPASS teleseismic model,
1010   Tectonophysics, 510, 195-206, doi: 10.1016/j.tecto.2011.07.001, 2011.

Moratto, L., Romano, M., Laurenzano, G., Colombelli, S., Priolo, E., Zollo, A., Saraò, A. and Picozzi, M.: Source parameter analysis of microearthquakes recorded around the underground gas storage in the Montello-Collalto Area (Southeastern Alps, Italy), Tectonophysics, 762, 159-168, doi: 10.1016/j.tecto.2019.04.030, 2019.

1015

Müller, W., Prosser, G., Mancktelow, N., Villa, I., Kelley, S., Viola, G. and Oberli, F.: Geochronological constraints on the evolution of the Periadriatic Fault System (Alps), International Journal of Earth Sciences, 90, 623-653, doi: 10.1007/s005310000187, 2001.

1020   Nussbaum, C.: Neogene tectonics and thermal maturity of sediments of the easternmost Southern Alps (Friuli area, Italy), PhD Thesis, Université de Neuchâtel, Switzerland, 172 pp., 2000.

Oldow, J., Bally, A. and Lallemant, H.: Transpression, orogenic float, and lithospheric balance, Geology, 18, doi: 10.1130/0091-7613(1990)018<0991:TOFALB>2.3.CO;2, 1990.

1025

Ortner, H., Aichholzer, S., Zerlauth, M., Pilser, R., Fügenschuh, B.: Geometry, amount and sequence of thrusting in the Subalpine Molasse of Western Austria and Southern Germany, European Alps, Tectonics, 34, doi: 10.1002/2014TC003550, 2015.

1030 Petersen, G. M., Cesca, S., Heimann, S., Niemz, P., Dahm, T., Kühn, D., Kummerow, J., Plenefisch, T., and the AlpArray Working Group: Regional centroid MT inversion of small to moderate earthquakes in the Alps using the dense AlpArray seismic network: challenges and seismotectonic insights, Solid Earth Discuss. [preprint], https://doi.org/10.5194/se-2021-13, in review, 2021.

1035 Picotti, V. and Cobianchi, M.: Jurassic stratigraphy of the Belluno Basin and Friuli Platform: a perspective on far-field compression in the Adria passive margin, Swiss Journal of Geosciences, doi: 10.1007/s00015-017-0280-5, 2017.

Picotti, V., Prosser, G. and Castellarin, A.: Structures and kinematics of the Giudicarie-Val Trompia fold and thrust belt (Central Southern Alps, Northern Italy), Mem. Sci. Geol., 47, 95-109, 1995.

1040

Picotti, V., Casolari, E., Castellarin, A., Mosconi, A., Cairo, E., Pessina, C. and Sella, M.: Alpine inversion of Mesozoic rift basin: the case of the Eastern Lombardian Prealps, AGIP-Universita di Bologna, 1-102, 1997.

Pilli, A., Sapigni, M. and Zuppi, G.: Karstic and alluvial aquifers: A conceptual model for the plain - Prealps system 1045 (northeastern Italy), Journal of Hydrology, s 464–465, 94–106, doi: 10.1016/j.jhydrol.2012.06.049, 2012.

Pomella, H., Urs, K., Scholger, R., Stipp, M. and Fügenschuh, B.: The Northern Giudicarie and the Meran-Mauls fault (Alps, Northern Italy) in the light of new paleomagnetic and geochronological data from boudinaged Eo-/Oligocene tonalites, International Journal of Earth Sciences, 100, 1827-1850, doi: 10.1007/s00531-010-0612-4, 2011.

1050

Pomella, H., Stipp, M. and Fügenschuh, B.: Thermochronological record of thrusting and strike-slip faulting along the Giudicarie Fault System (Alps, Northern Italy), Tectonophysics, 579, 118-130, doi: 10.1016/j.tecto.2012.04.015, 2012.

1055 Pola, M., Ricciato, A., Fantoni, R., Fabbri, P. and Zampieri, D.: Architecture of the western margin of the North Adriatic foreland: The Schio-Vicenza fault system, Italian Journal of Geosciences, 133, 223-234, doi: 10.3301/IJG.2014.04, 2014.

Pola, M., Fabbri, P., Piccinini, L., Zampieri, D.: Conceptual and numerical models of a tectonically-controlled geothermal system: A case study of the Euganean Geothermal System, Northern Italy, Central European Geology, 58, 129-150, doi: 10.1556/24.58.2015.1-2.9, 2015.

Prosser, G.: Strike-slip movements and thrusting along a transpressive fault zone: The North Giudicarie line (Insubric line, Northern Italy), Tectonics, 17, 921-937, doi: 10.1029/1998TC900010, 1998.

Prosser, G.: The development of the North Giudicarie fault zone (Insubric Line, Northern Italy), Journal of Geodynamics, 30, 229-250, doi: 10.1016/S0264-3707(99)00035-6, 2000.

Qorbani, E., Bianchi, I. and Bokelmann, G.: Slab detachment under the Eastern Alps seen by seismic anisotropy, Earth and Planetary Science Letters, 409, 96-108, doi: 10.1016/j.epsl.2014.10.049, 2015.

Ratschbacher, L., Frisch, W., Neubauer, F., Schmid, S. and Neugebauer, J.: Extension in compressional orogenic belts: The Eastern Alps, Geology, doi: 7613217. 404-407. 10.1130/0091-7613(1989)017<0404:EICOBT>2.3.CO;2, 1989.

Ratschbacher, L., Frisch, W., Linzer, H. and Merle, O.: Lateral extrusion in the eastern Alps, Part 2: Structural analysis, Tectonics, 10, 257-271, doi: 10.1029/90TC02623, 1991.

Reverman, R., Fellin, M., Herman, F., Willett, S., and Fitoussi, C.: Climatically versus tectonically forced erosion in the Alps Thermochronometric constraints from the Adamello Complex, Southern Alps, Italy, Earth and Planetary Science Letters, 339-340, 127-138, doi: 10.1016/j.epsl.2012.04.051, 2012.

Roeder, D. (1992).: Thrusting and wedge growth, Southern Alps of Lombardia (Italy), Tectonophysics, 207, 199-243, doi: 10.1016/0040-1951(92)90478-O, 1992.

Romano, M. A., Peruzza, L., Garbin, M., Priolo, E., and Picotti, V.: Microseismic Portrait of the Montello Thrust (Southeastern Alps, Italy) from a Dense High-Quality Seismic Network, Seismological Research Letters, 90, 1502–1517, 2019.

Rosenberg, C. and Garcia, S.: Estimating displacement along the Brenner Fault and orogen-parallel extension in the Eastern Alps, Int. J. Earth Sci., 100, 1129-1145, doi: 10.1007/s00531-011-0645-3, 2011.

Rosenberg, C., Kissling, E.: Three-dimensional insight into Central-Alpine collision: Lower-plate or upper-plate indentation?, Geology, 41, 1219-1222, doi: 10.1130/G34584.1, 2013.

Rosenberg, C. and Schneider, S.: The western termination of the SEMP Fault (eastern Alps) and its bearing on the exhumation of the Tauern Window, Geological Society, London, Special Publications, 298, 197-218, doi: 10.1144/SP298.10, 2008.

1100   Rosenberg, C., Brun, J., Cagnard, F. and Gapais, D.: Oblique indentation in the Eastern Alps: Insights from laboratory experiments, Tectonics, 26, doi: 10.1029/2006TC001960, 2007.

Rosenberg, C., Schneider, S., Scharf, A., Bertrand, A., Hammerschmidt, K., Rabaute, A. and Brun, J.: Relating collisional kinematics to exhumation processes in the Eastern Alps, Earth-Science Reviews, 176,
1105   10.1016/j.earscirev.2017.10.013, 2018.

Scharf, A., Handy, M., Favaro, S., Schmid, S. and Bertrand, A.: Modes of orogen-parallel stretching and extensional exhumation in response to microplate indentation and roll-back subduction (Tauern Window, Eastern Alps), International Journal of Earth Sciences, 102, doi: 10.1007/s00531-013-0894-4, 2013.

1110

Schmid, S., Kissling, E.: The arc of the Western Alps in the light of new data on deep crustal structure, Tectonics, 19, doi: 62-85. 10.1029/1999TC900057, 2000.

Schmid, S., Pfiffner, O., Kissling, E., Froitzheim, N. and Schönborn, G.: Geophysical-geological transect and tectonic
1115   evolution of the Swiss-Italian Alps, Tectonics, 15, 1036-1064, doi: 10.1029/96TC00433, 1996.

Schmid, S., Fügenschuh, B., Kissling, E. and Schuster, R.: Tectonic map and overall architecture of the Alpine orogeny, Eclogae Geologicae Helvetiae, 97, 93-117, doi: 10.1007/s00015-004-1113-x, 2004.

1120   Schmid, S., Bernoulli, D., Fügenschuh, B., Matenco, L., Schefer, S., Schuster, R., Tischler, M. and Ustaszewski, K.: The Alpine-Carpathian-Dinaridic orogenic system: Correlation and evolution of tectonic units, Swiss Journal of Geosciences, 101, 139-183, doi: 10.1007/s00015-008-1247-3, 2008.

Schmid, S., Scharf, A., Handy, M. and Rosenberg, C.: The Tauern Window (Eastern Alps, Austria): A new tectonic
1125   map, with cross-sections and a tectonometamorphic synthesis, doi: 10.1007/s00015-013-0123-y, 2013.

Schönborn, G.: Alpine Tectonics and kinematic models of the central southern Alps, Mem. Sci. Geol., 44, 1992.

Schönborn, G.: Balancing cross sections with kinematic constraints: The Dolomites (northern Italy), Tectonics, 18,
1130   527-545, doi: 10.1029/1998TC900018, 1999.

Selli, L.: Il lineamento della Valsugana fra Trento e Cima d'Asta: cinematica neogenica ed eredità strutturali permo-mesozoiche nel quadro evolutivo del Sudalpino Orientale (NE-Italia), Mem. Soc. Geol. It, 53, 503-541, 1998.

1135 Selli, L., Bargossi, G., Battistini, G., Mordenti, A., Tranne, C. and Stefani, A.: Le vulcaniti permiane a N della Linea del Calisio: Evoluzione strutturale del margine SW del distretto vulcanico atesino (Trento, Italia), Mineralogica et Petrographica Acta, 169-196, 1996.

Semenza, E.: La fase Giudicariense, nel quadro di una nuova ipotesi sull'Orogenesi Alpina nell'area Italo-Dinarica,
1140 Mem. Soc. Geol. It., 13, 187-226, 1974.

Serpelloni, E., Vannucci, G., Anderlini, L. and Bennett, R.: Kinematics, seismotectonics and seismic potential of the eastern sector of the European Alps from GPS and seismic deformation data, Tectonophysics, 688, doi: 10.1016/j.tecto.2016.09.026, 2016.

1145

Spada, M., Bianchi, I., Kissling, E., Agostinetti, N. and Wiemer, S.: Combining controlled-source seismology and receiver function information to derive 3-D Moho topography for Italy, Geophysical Journal International, 194, 1050-1068, doi: 10.1093/gji/ggt148, 2013.

1150 Stipp, M., Fügenschuh, B., Gromet, L., Stünitz, H. and Schmid, S.: Contemporaneous plutonism and strike-slip faulting: A case study from the Tonale fault zone north of the Adamello pluton (Italian Alps), Tectonics, 23, doi: TC3004. 10.1029/2003TC001515, 2004.

Suppe, J.: Geometry and Kinematics of Fault-bend Folding, American Journal of Science, 283, 684-721, 1983.

1155

Tapponnier, P., Peltzer, G. and Armijo, R.: On the mechanics of the collision between India and Asia, Geological Society, London, Special Publications, 19, 113-157, doi: 10.1144/GSL.SP.1986.019.01.07, 1986.

Thöny, W., Ortner, H., Scholger, R.: Paleomagnetic evidence for large en-bloc rotations in the Eastern Alps during
1160 Neogene orogeny, Tectonophysics, 414, doi: 10.1016/j.tecto.2005.10.021, 2006.

Ustaszewski, K., Schmid, S., Fügenschuh, B., Tischler, M., Kissling, E. and Spakman, W.: A map-view restoration of the Alpine-Carpathian-Dinaridic system for the Early Miocene, Swiss Journal of Geosciences, 101, 273-294, doi: 10.1007/s00015-008-1288-7, 2008.

1165

Van Hinsbergen, D., Torsvik, T., Schmid, S., Maţenco, L., Maffione, M., Vissers, R., Gürer, D. and Spakman, W.: Orogenic architecture of the Mediterranean region and kinematic reconstruction of its tectonic evolution since the Triassic, Gondwana Research, 81, 79-229, doi: 10.1016/j.gr.2019.07.009, 2020.

1170   Verwater, V.F., Le Breton, E., Handy, M.R., Picotti, V., Jozi Najafabadi, A. and Haberland, C.: Balanced cross sections along the Giudicarie Belt (Southern Alps, Northern Italy) in 3-D Move, GFZ Data Services, doi: https://doi.org/10.5880/fidgeo.2021.006, 2021.

        Viganò, A., Scafidi, D., Ranalli, G., Martin, S., Vedova, B. D., and Spallarossa, D.: Earthquake relocations, crustal
1175   rheology, and active deformation in the central–eastern Alps (N Italy), Tectonophysics, 661, 81 – 98, 2015.

        Viganò, A., Zampieri, D., Rossato, S., Martin, S., Selli, L., Prosser, G., Ivy-Ochs, S., Campedel, P., Fedrizzi, F., Franceschi, M., and Rigo, M.: Past to present deformation of the central-eastern Southern Alps: from the foreland to the Giudicarie belt, Geological Field Trips and Maps, 10, 1-78, doi: 10.3301/GFT.2018.01, 2018.
1180
        Viola, G., Mancktelow, N. and Seward, D.: Late Oligocene-Neogene evolution of Europe-Adria collision: New structural and geochronological evidence from the Giudicarie fault system (Italian Eastern Alps), Tectonics, 20, 999-1020, doi: 10.1029/2001TC900021, 2001.

1185   Von Hagke, C., Cederbom, C., Oncken, O., Stockli, D., Rahn, M. and Schlunegger, F.: Linking the Northern Alps with Their Foreland: the Latest Exhumation History Resolved by Low-Temperature Thermochronology, Tectonics, 31, doi: 10.1029/2011TC003078, 2012.

        Winterer, E. and Bosellini, A.: Subsidence and sedimentation on Jurassic passive continental margin, Southern Alps,
1190   Italy, AAPG Bulletin, 65(3), 394-421, 1981.

        Zampieri, D.: Tertiary extension in the Southern Trento Platform, Southern Alps, Italy, Tectonics, 14, 645-657, doi: 10.1029/94TC03093, 1995.

1195   Zampieri, D., Massironi, M., Sedea, R. and Sparacino, V.: Strike-slip contractional stepovers in the Southern Alps (Northeastern Italy), Eclogae Geologicae Helvetiae, 96, 115-123, 2003.

        Zampieri, D., Vannoli, P., and Burrato, P.: Geodynamic and seismotectonic model of a long-lived transverse structure: The Schio-Vicenza Fault System (NE Italy), Solid Earth Discuss. [preprint], https://doi.org/10.5194/se-2021-29, in
1200   review, 2021.

        ViDEPI Project https://www.videpi.com/videpi/videpi.asp last access: 11 May 2021